

We thank the anonymous referee for his/her comments. We would like to remark that the referee erroneously reviewed the original version of the manuscript instead of the revised version. Therefore, some comments do not apply anymore. Below please find a point by point reply to all comments, with our replies marked as “RESPONSE”. The changes made in the original manuscript are highlighted in yellow. A marked-up manuscript version is attached.

REFEREE: Dear Editor,

Grimmer et al. present palynological and geochemical data tracing hydrological changes from western equatorial South America during the early Pliocene. Given the existing uncertainties of Pliocene climate variability, the controversial discussed shift of the ITCZ possibly in response to the CAS closure, and existing discrepancy between paleoceanographic and model data I feel that the presented study makes a valuable and important contribution to the community. Generally, I consider the manuscript well written, the discussion poses interesting questions and it should be considered for publication after minor revisions.

From the replies to the previous and detailed reviews I find that the authors have addressed the majority of raised issues. However, some concerns remain for me related to the age model in line with previous reviewer suggestions. I find this crucial part of the study is too briefly discussed and I would like to invite the authors to provide a more in-depth description of what was actually done. I think this is crucial aspect of this study as their new insights into i.e. the onset of the ITCZ shift, easterly wind intensification and ENSO variability requires a firm age constrain. Thus, things I would like to know are: how many, if any, of the stated biostratigraphic maker fall into the study time frame (4.2.-4.7 Ma), and can thus provide direct age control?

RESPONSE: The identified pollen and spores were not used as biostratigraphic markers, because the oxygen isotope stratigraphy of the applied age model (Tiedemann et al. 2007) provides more precise age constraints.

REFEREE: Where are the referenced benthic stable isotope derived from? No citation is provided in Line 200 about these stable isotope data thus I am to assume this is data has been measured in relation to this study? If so, why is this data and its underlying methodologically not properly included and discussed?

RESPONSE: The benthic stable isotopes were measured by Tiedemann et al. (2007) as referenced in the following sentence (line 206). To make it more clear, **another reference was included in line 205.**

REFEREE: Why is there no age model figure provided in the supplements or main text to highlight the visually correlation, the biostratigraphic events included in the time frame and sedimentation rates?

RESPONSE: We included a new figure with the age-depth model as supplementary material (Fig. S2).

REFEREE: How did the authors establish that 5 m hiatus relate to roughly 100 kyr? Is this hiatus caused by bottom current changes, turbidites, core loss etc.? Sedimentation rate patterns before and after the hiatus might provide an insight into this question. If bottom current changes play a role could this cause to a bias to the pollen assemblage preserved?

RESPONSE: The age-depth correlation was established by Tiedemann et al. (2007). We simply used linear interpolation to calculate the age of the gap. In the initial version of the manuscript, the gap was erroneously described as “hiatus”, but this has been changed to “coring gap”, which implies that there is no general lack in the sediment sequence caused by bottom current changes, turbidites etc., but rather a sediment loss during coring (this is, however, only an assumption because no details about the coring gap are given in the original publication (Tiedemann et al. 2007)).

REFEREE: Minor issues:

Lines: 114, 115, 119, 130-135, 162-167, 172-174, 177 please provide proper citations for the information provided in these lines.

RESPONSE: Lines 114, 115: Citations were included already in the previous revision (new version line 110). Line 119: The citation is given after the following sentence (new version line 116). Lines 130-135: The citation “Balslev 1988” was moved from line 124 to line 126 to include lines 124-126. Another citation was added (new version line 129). Lines 162-167: A citation was added in line 159. Lines 172-174: A citation was added in line 171. Line 177: The sentence was deleted because it was redundant.

REFEREE: Lines 175-178: It seems to me that 150-200 km paleo-distance seems a bit far to call this site a direct recorder of fluvial input.

RESPONSE: Other studies of the same site (Rincón-Martínez et al. 2010) and same region (González et al. 2006) have shown that the terrestrial fluvial signal is recorded in the marine sediments. One sediment core analyzed by González et al. is even located twice as far from the shore (400 km).

REFEREE: The Fe/K is used as a tracer of fluvial input but those seem rather mild throughout the whole investigated interval whereas the pollen-based indicator of humid conditions shows much more high amplitude variability. What can cause the dissimilarities?

RESPONSE: The differences in amplitude between the proxies are small. The changes in vegetation are rather subtle as well, which we mention several times (compare lines 20, 339, 496). Fe/K and the pollen group of humid indicators are both used to infer changes in fluvial runoff, but it must be considered that their amplitudes of change cannot be directly compared. There are other hydrological effects which might play a role (e.g. the indicators of humid conditions may also record higher soil moisture which is not necessarily coupled with higher fluvial runoff).

REFEREE: Since you also discussed the possibility of eolian transport of pollen (Lines 342ff) how would that relate to river run off changes at the same time?

RESPONSE: This relation is described in section 4.3.2. When pollen transport is only fluvial, high precipitation and runoff would coincide with high pollen concentrations. As this is not the case in pollen zone III where the pollen concentration is high despite less humid conditions, additional eolian transport is considered (compare also Fig. 4).

REFEREE: Lines 179: Isn't the Guayas River a bit far south to be directly linked to Site 1239?

RESPONSE: ODP Site 1239 was also located further south in the Pliocene (compare line 172). Additionally, it was also shown by Rincón-Martínez et al. 2010 that the fluvial signal of the Guayas River is captured by Site 1239.

REFEREE: Lines 182: Please state the mcd depth interval that was investigated as this is not immediately obviously from just stating the core numbers.

RESPONSE: The mbsf depth interval was already added during the previous review phase (line 186).

REFEREE: Lines 182: the modern analogue sample were taken how?

RESPONSE: The modern analogue samples were taken the same way as the other samples.

REFEREE: Lines 201: Please explain what you mean by “indirectly orbital tuned”?

RESPONSE: **An explanation was added in line 205.**

REFEREE: Line 206: How sampled? U-channels, full cores or discrete samples? I suggest you change “A” to “This”.

RESPONSE: The measurements were done on the split cores with a non-destructive technique as described in lines 209-214 and references therein. We prefer to stick with “A”.

REFEREE: Line 202: mcd depth of hiatus?

RESPONSE: The information was added (new version line 207).

REFEREE: Line 209: A question for me also remains whether or not the XRF-data was corrected for dead time and sample geometry effects? What about non-linear matrix effects? Also, you state Ca alongside Fe and K but never pick up on it during the discussion? Why did you not use Ti/Ca for terrigenous influx/marine productivity since insights into marine productivity changes might also hold information on ocean circulation changes in relation to i.e. ENSO?

RESPONSE: The data was corrected for dead time. The information was added in line 210. Sample geometry effects and non-linear matrix effects were not considered because it does not apply to the measurement technique. In the methods section, Ca was mentioned as an example when describing the technique. In order to not confuse the reader, the examples of elements in line 212 (“such as Fe, Ca, and K”) were removed. We used Fe/K as a tracer for fluvial input, because our study focusses on terrestrial changes in hydrology. The use of Ti/Ca for terrestrial climate reconstructions is problematic as Ca is sensitive to dilution effects.

REFEREE: Line 334: unpublished data by whom?

RESPONSE: Our own data, which has already been included in the revised version.

# Early Pliocene vegetation and hydrology changes in western equatorial South America

Friederike Grimmer<sup>1</sup>, Lydie Dupont<sup>1</sup>, Frank Lamy<sup>2</sup>, Gerlinde Jung<sup>1</sup>, Catalina González<sup>3</sup>, Gerold Wefer<sup>1</sup>

<sup>1</sup>MARUM – Center for Marine Environmental Sciences, University of Bremen, Leobener Str. 8, 28359 Bremen, Germany

<sup>2</sup>Alfred-Wegener-Institute for Polar and Marine Research, Am Handelshafen 12, 27570 Bremerhaven, Germany

<sup>3</sup>Department of Biological Sciences, Universidad de los Andes, Cra. 1 #18a-12, Bogotá, Colombia

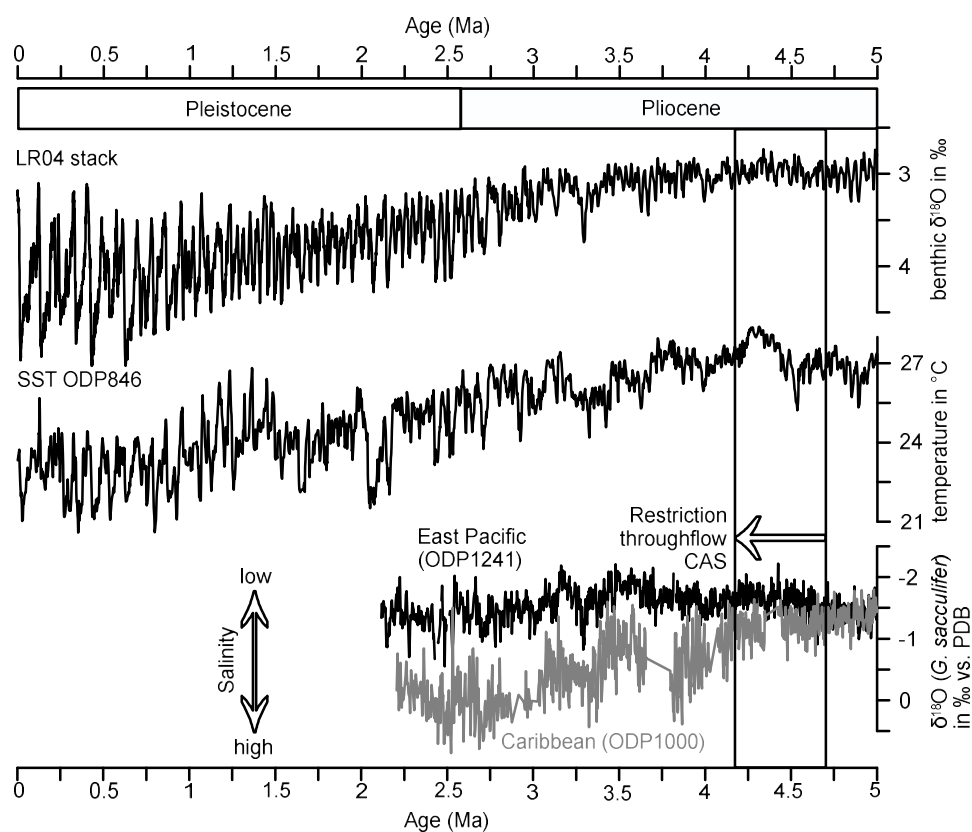
Correspondence to: Friederike Grimmer (fgrimmer@marum.de)

**Abstract.** During the early Pliocene, two major tectonic events triggered a profound reorganization of ocean and atmospheric circulation in the Eastern Equatorial Pacific (EEP), the Caribbean Sea, and on adjacent land masses: the progressive closure of the Central American Seaway (CAS) and the uplift of the northern Andes. These affected amongst others the mean latitudinal position of the Intertropical Convergence Zone (ITCZ). The direction of an ITCZ shift however is still debated, as numeric modelling results and paleoceanographic data indicate shifts in opposite directions. To provide new insights into this debate, an independent hydrological record of western equatorial South America was generated. Vegetation and climate of this area were reconstructed by pollen analysis of 46 samples from marine sediments of ODP Hole 1239A from the EEP comprising the interval between 4.7 and 4.2 Ma. The study site is sensitive to latitudinal ITCZ shifts insofar as a southward (northward) shift would result in increased (decreased) precipitation over Ecuador. The presented pollen record comprises representatives from five ecological groups: lowland rainforest, lower montane forest, upper montane forest, páramo, and broad range taxa. A broad tropical rainforest coverage persisted in the study area throughout the early Pliocene, without significant open vegetation beyond the páramo. Between 4.7 and 4.42 Ma, humidity increases, reaching its peak around 4.42 Ma, and slightly decreasing again afterwards. The stable, permanently humid conditions are rather in agreement with paleoceanographic data indicating a southward shift of the ITCZ, possibly in response to CAS closure. The presence of páramo vegetation indicates that the Ecuadorian Andes had already reached considerable elevation by the early Pliocene. Future studies could extend the hydrological record of the region further back into the late Miocene to see if a more profound atmospheric response to tectonic changes occurred earlier.

## 1 Introduction

The progressive closure of the Central American Seaway (CAS) and the uplift of the northern Andes profoundly reorganized early Pliocene ocean and atmospheric circulation in the Eastern Equatorial Pacific (EEP). The formation of the Isthmus of Panama, and especially the precise temporal constraints of the closure of the Panama Strait, have been subject of numerous studies (Bartoli et al., 2005; Groeneveld et al., 2014; Hoorn and Flantua, 2015; Montes et al., 2015; Steph, 2005). A recent review based on geological, paleontological, and molecular records narrowed the formation *sensu stricto* down to 2.8 Ma (O’Dea et al., 2016). Temporal constraints on the restriction of the surface water flow through the gateway were established by salinity reconstructions on both sides of the Isthmus (Steph et al., 2006b, Fig. 1). The salinities first start to diverge around 4.5 Ma. A major step in the seaway closure between 4.7 and 4.2 Ma was also assumed based on the comparison of mass accumulation rates of the carbonate sand-fraction in the Caribbean Sea and the EEP (Haug and Tiedemann, 1998). The closure of the Central American Seaway has been associated with the development of the EEP cold tongue (EEP CT), strengthened upwelling in the EEP, the shoaling of the thermocline, and a mean latitudinal shift of the Intertropical Convergence Zone (ITCZ; (Steph, 2005; Steph et al., 2006a; Steph et al., 2006b; Steph et al., 2010). The direction of a potential shift of the ITCZ is still debated because of a discrepancy between paleoclimate reconstructions based on proxy data and numerical modelling results.

40 For the late Miocene, a northernmost paleoposition of the ITCZ at about 10–12°N has been proposed (Flohn, 1981; Hovan,  
 41 1995). Subsequently, a southward shift towards 5°N paleolatitude between 5 and 4 Ma is indicated by eolian grain-size  
 42 distributions in the eastern tropical Pacific (Hovan, 1995). Billups et al. (1999) provide additional evidence for a southward  
 43 shift of the ITCZ between 4.4 and 4.3 Ma. Hence, most proxy data agree about a southward ITCZ shift during the early  
 44 Pliocene. On the contrary, results from numerical modelling suggest a northward shift of the ITCZ in response to CAS closure  
 45 (Steph et al., 2006b) and Andean uplift (Feng and Poulsen, 2014; Takahashi and Battisti, 2007).  
 46 An independent record of the terrestrial hydrology for the early Pliocene from a study site that is sensitive to latitudinal ITCZ  
 47 shifts could provide new insights to this debate. Schneider et al. (2014) also stress the need of reconstructions of the ITCZ in  
 48 the early and mid-Pliocene in order to understand how competing effects like an ice-free northern hemisphere and a weak EEP  
 49 CT balanced, and to reduce uncertainties of predictions. Even though changes of ocean–atmosphere linkages related to ENSO  
 50 (El Niño Southern Oscillation) and ITCZ shifts strongly impact continental precipitation in western equatorial South America,  
 51 most studies so far have focused on paleoceanographic features such as sea-surface temperatures and ocean stratification.



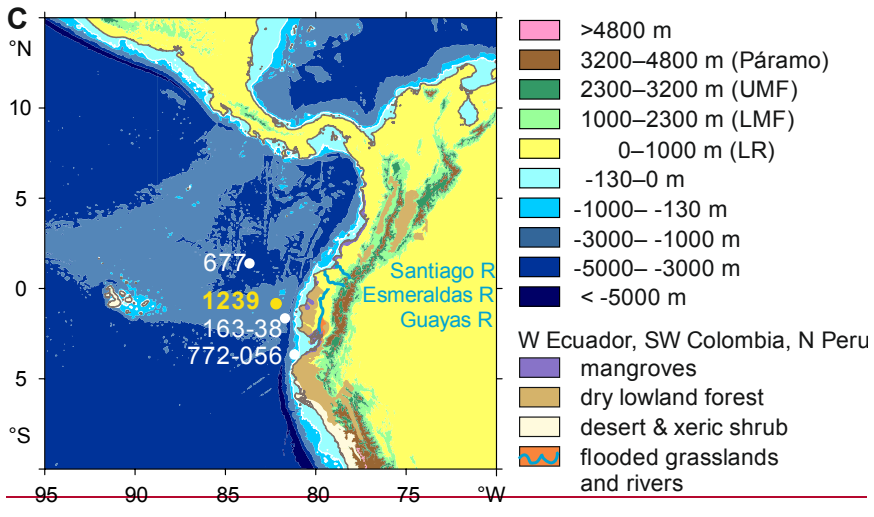
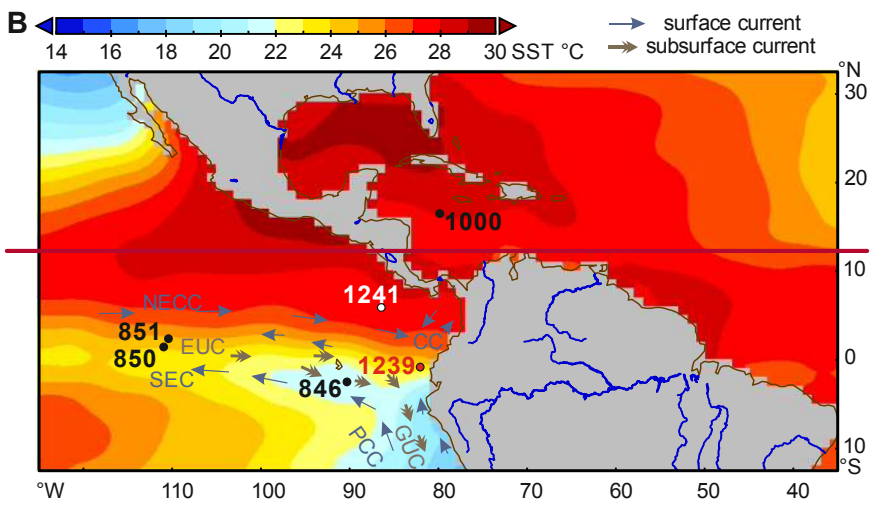
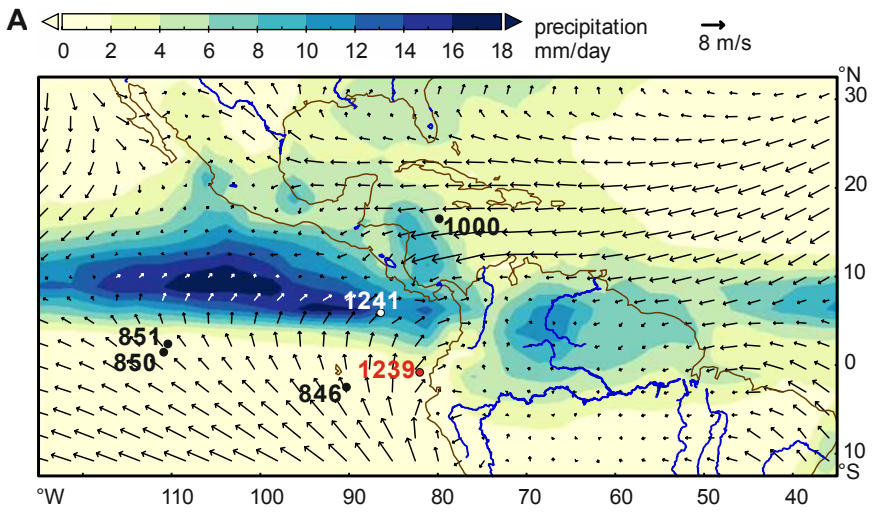
52  
 53 **Figure 1. LR04 global stack of benthic  $\delta^{18}\text{O}$  reflecting changes in global ice volume and temperature (Lisiecki and Raymo, 2005).**  
 54 **UK<sub>37</sub> sea-surface temperatures (SST) of ODP Site 846 in the Equatorial Pacific Cold Tongue (Lawrence et al., 2006).  $\delta^{18}\text{O}$  of the**  
 55 **planktonic foraminifer *G. sacculifer* from ODP Site 1000 in the Caribbean and ODP Site 1241 in the East Pacific (Haug et al., 2001;**  
 56 **Steph, 2005; Steph et al., 2006a), reflecting changes in sea-surface salinity (see Fig. 2 for location of ODP Sites). The box represents**  
 57 **the time window analyzed in this study.**

58  
 59 The second major tectonic process is the uplift of the northern Andes which strongly altered atmospheric circulation patterns  
 60 over South America. Three major deformation phases include fan building in the lower Eocene to early Oligocene,  
 61 compression of Oligocene deposits in the Miocene and Pliocene, and refolding during Pliocene to recent times (Corredor,  
 62 2003). While the uplift of the Central Andes is well investigated, only few studies deal with the timing of uplift of the northern  
 63 Andes. Coltorti and Ollier (2000), based on geomorphologic data, conclude that the uplift of the Ecuadorian Andes started in  
 64 the early Pliocene and continued until the Pleistocene. More recent apatite fission track data indicate that the western Andean  
 65 Cordillera of Ecuador was rapidly exhumed during the late Miocene (13–9 Ma) (Spikings et al., 2005). Uplift estimates for the  
 66 Central Andes suggest that the Altiplano had reached less than half of its modern elevation by 10 Ma, with uplift rates

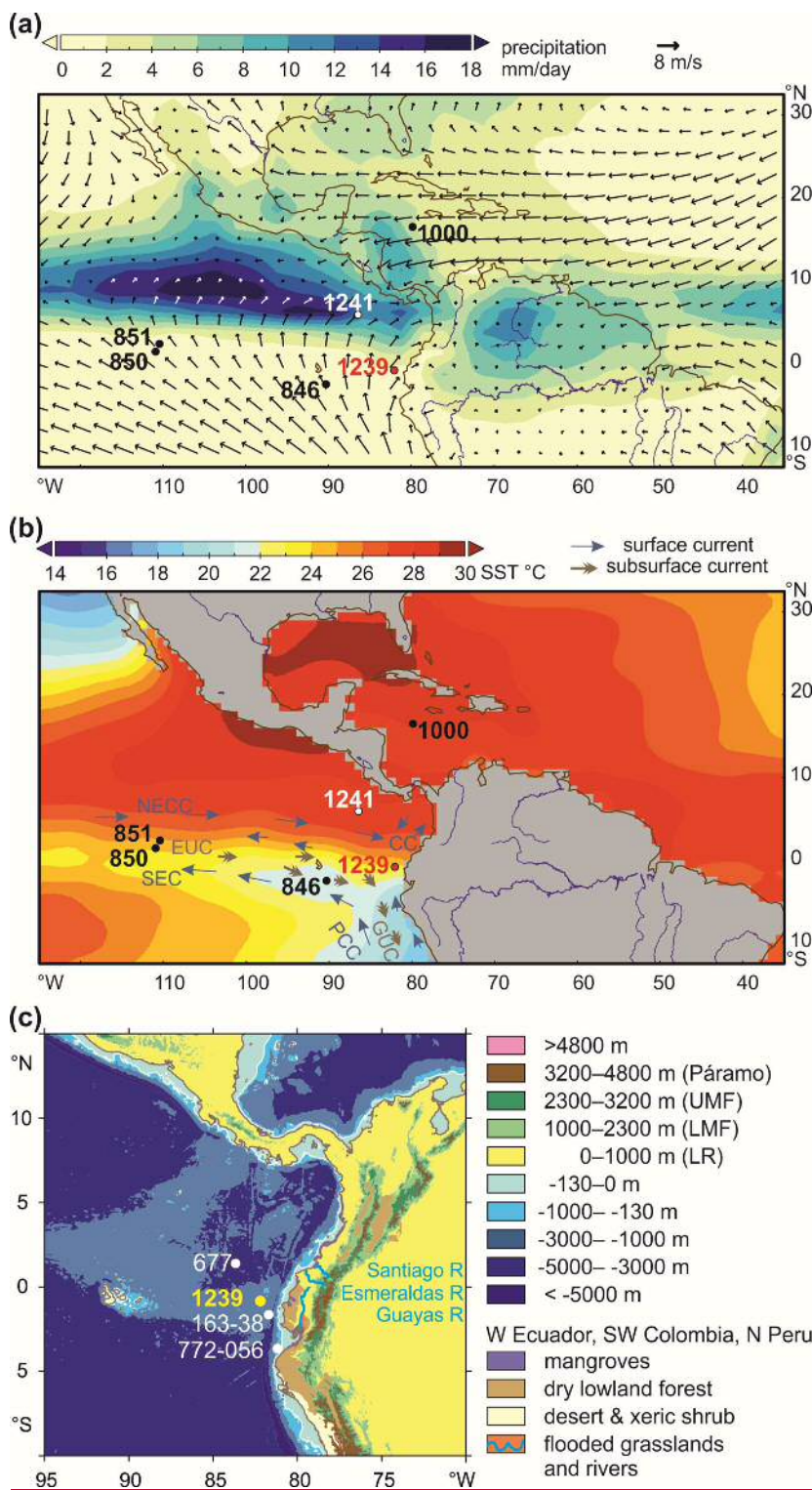
67 increasing from 0.1 mm/yr in the early and middle Miocene to 0.2–0.3 mm/yr to present. For the Eastern Cordillera of  
68 Colombia, elevations of less than 40% of the modern values are estimated for the early Pliocene, then increasing rapidly at  
69 rates of 0.5–3 mm/yr until modern elevations were reached around 2.7 Ma (Gregory-Wodzicki, 2000). Both the tectonic events  
70 and the closure of the Central American Seaway are assumed to have had a large impact on ocean and atmospheric circulation  
71 in the eastern Pacific, the Caribbean and on adjacent land masses. Therefore, the reconstruction of continental climate,  
72 especially hydrology, will contribute to our understanding of climatic changes in this highly complex area.

73 To better understand the early Pliocene vegetation and hydrology of western equatorial South America we studied pollen and  
74 spores from the early Pliocene section (4.7–4.2 Ma) of the marine sediment record at ODP Site 1239 and compared this record  
75 to Holocene samples from the same Site. In addition, we use elemental ratios to estimate variations in fluvial terrestrial input  
76 (Rincon-Martínez et al. 2010). While other palynological studies of the region have been conducted for the mid-Pliocene to  
77 Holocene (González et al., 2006; Hooghiemstra, 1984; Seilles et al., 2016), only a few palynological records for the early  
78 Pliocene exist (Wijninga and Kuhry, 1990; Wijninga, 1996). The record contributes to elucidate how vegetation and climate  
79 in this area responded to changes in atmospheric and oceanic circulation, possibly induced by the closure of the Central  
80 American Seaway and the uplift of the northern Andes. Therefore the main objectives of the study are firstly, to investigate  
81 long-term vegetation and climatic changes, focusing on hydrology, in western equatorial South America and, secondly, to  
82 interpret these changes in relation to climate phenomena influencing the hydrology of the region, especially the mean  
83 latitudinal position of the ITCZ and variability related to ENSO. These objectives are approached by the following research  
84 questions: 1) What floral and vegetation changes took place in the coastal plain of western equatorial South America and the  
85 Ecuadorian Andes from 4.7 to 4.2 Ma? 2) What are the climatic implications of the vegetation change, especially in terms of  
86 hydrology? 3) What are the implications for Andean uplift, especially regarding the development of the high Andean páramo  
87 vegetation?

88







90

91 **Figure 2. Modern climate (boreal summer) and vegetation and core site positions of ODP Sites 677, 846, 850, 851, 1000, 1239, 1241,**  
 92 **Trident core TR163-38, and M772-056 mentioned in the text. A. Long-term monthly July precipitation in mm/day (CPC) and wind**  
 93 **field (NCEP). July is the middle of the rainy season in northern South America, when the ITCZ is at its northern boreal summer**  
 94 **position. Salinity estimates for the Caribbean indicate a position of the ITCZ further north during the Pliocene. Direction of wind is**  
 95 **not favorable for wind transport of pollen and spores to ODP Site 1239. B. Long-term monthly July sea-surface temperatures**  
 96 **(NODC), surface and subsurface currents of the eastern equatorial Pacific (Mix et al. 2003). NECC, North Equatorial**  
 97 **Countercurrent; SEC, South Equatorial Current; PCC, Peru-Chile Current (continuation of the Humboldt Current); CC, Coastal**  
 98 **Current; EUC, Equatorial Undercurrent; GUC, Gunther Undercurrent. C. Contours, bathymetry (ETOPO1), main rivers in**  
 99 **Ecuador, and vegetation. Transport of pollen and spores in the ocean over the Peru-Chile Trench, which is very narrow east of the**  
 100 **Carnegie Ridge, probably takes place in nepheloid layers. Páramo vegetation is found between 3200 and 4800 m, upper montane**  
 101 **Andean forest (UMF) grows between 1000 and 2300 m, sub-Andean lower montane forest (LMF) between 1000 and 2300 m, and**  
 102 **lowland forest (LR) below 1000m. The distribution of desert and xeric shrubs in northern Peru, drier broad-leaved forest, flooded**  
 103 **grasslands, and mangroves in Ecuador and Colombia is denoted in different colors (see legend, WWF). Source areas of pollen and**  
 104 **spores in sediments of ODP Site 1239 are sought in western Ecuador, northwestern Peru, and southwestern Colombia (see text).**  
 105 **Abbreviated web sources and retrieval dates are listed under references.**

## 107 1.1 Modern setting

### 108 1.1.1 Climate and ocean circulation

109 The climate of western equatorial South America is complex and heterogeneous, as it is not only controlled by large-scale  
 110 tropical climate phenomena such as the ITCZ and ENSO, but is also strongly influenced by small-scale climate patterns caused  
 111 by the diverse Andean topography (Marchant et al., 2001; Niemann et al., 2010). The annual cycle of precipitation in  
 112 northwestern South America is controlled by insolation changes. During boreal summer when insolation is strongest in the  
 113 northern hemisphere, the ITCZ is located at its northernmost position around 9°–10° N (Vuille et al., 2000). Approaching  
 114 austral summer, the ITCZ moves southward across the equator. Within the range of the ITCZ, annual precipitation patterns are  
 115 generally characterized by two minima and two maxima. The coastal areas of southern Ecuador where the ITCZ has its  
 116 southernmost excursion show an annual precipitation pattern with one maximum during austral summer and a pronounced dry  
 117 season during austral winter (Bendix and Lauer, 1992).

118 This general circulation pattern is modified by ENSO at interannual time-scales. During warm El Niño events, the lowlands  
 119 of Ecuador experience abundant precipitation whereas the northwestern Ecuadorian Andes experience drought (Vuille et al.,  
 120 2000). Regional climate patterns are also modified by the topography of the Andes which pose an effective barrier for the  
 121 large-scale atmospheric circulation. While precipitation patterns east of the Andes are driven by moisture-laden easterly trade  
 122 winds originating over the tropical Atlantic and the Amazon basin, the coastal areas and the western Andean slopes are  
 123 dominated by air masses originating in the Pacific (Vuille et al., 2000, Fig. 2). The warm annual El Niño current which flows  
 124 southward along the Colombian Pacific coast warms the air masses along the coast. This moist air brings over 6000 mm yearly  
 125 precipitation to the northern coastal plain (Balslev, 1988). In contrast, the coastal areas of southernmost Ecuador and northern  
 126 Peru are under the influence of the Peru-Chile Current, which is a continuation of the cold Humboldt Current transporting cold  
 127 and nutrient rich waters and giving rise to a long strip of coastal desert (Balslev, 1988). The westwards flow of the cold surface  
 128 waters of the EEP CT to the western Pacific via the South Equatorial Current (SEC) is driven by the Walker Circulation. Warm  
 129 waters return eastwards via the North Equatorial Countercurrent (NECC, see Fig. 2). An abrupt transition between the cold  
 130 SEC and the warm NECC is the Equatorial Front (EF) (EF, Pak and Zaneveld, 1974).

### 131 1.1.2 Geography, vegetation and pollen transport

132 Ecuador is geographically divided into three main regions: the coastal plain with several rivers draining into the Pacific, the  
 133 Andes, and the eastern lowlands which constitute the western margin of the Amazon Basin. The mountains form two parallel  
 134 cordilleras which are separated by the Interandean Valley. The diverse vegetation is the result of the combined effects of  
 135 elevation and precipitation. In the coastal plain there is an abrupt shift from tropical lowland rainforests in the north to a desert  
 136 dominated by annual xerophytic herbs in the south. This shift reflects the dependence of the vegetation on precipitation which  
 137 ranges from 100 to 6000 mm per year on the coastal plain. The western slopes of the Andes are covered by montane forest,  
 138 which is partly interrupted by drier valleys in southern Ecuador (Balslev, 1988).

139 Along the coast, mangrove stands occur in the salt- and brackish-water tidal zone of river estuaries and bays. They are formed  
 140 by two species of *Rhizophora* (*R. harrisonii* and *R. mangle*), and to a lesser extent *Avicennia*, *Laguncularia*, and *Conocarpus*  
 141 are present (Twilley et al., 2001). The lowland rainforest is characterized by the dominant plant families Fabaceae, Rubiaceae,  
 142 Arecaceae, Annonaceae, Melastomataceae, Sapotaceae, and Clusiaceae in terms of species richness. In the understory,  
 143 Rubiaceae, Araceae, and Piperaceae form the predominant elements (Gentry, 1986). In the lower montane forest, *Cyathea*,  
 144 Meliaceae (e.g. *Ruagea*), Fabaceae (e.g. *Dussia*), Melastomataceae (e.g. *Meriania*, *Phainantha*), Rubiaceae (e.g. *Cinchona*),  
 145 Proteaceae (e.g. *Roupala*), Lauraceae (e.g. *Nectandra*), and Pteridaceae (e.g. *Pterozonium*) are common elements. Upper  
 146 montane forests are dominated by *Myrsine*, *Ilex*, *Weinmannia*, *Clusia*, *Schefflera*, *Myrcianthes*, *Hedyosmum*, and *Oreopanax*

147 (Jørgensen et al., 1999). Above ca. 3200 m, trees become sparse and eventually the vegetation turns into páramo. The páramo  
148 is a unique ecosystem of the high altitudes of the northern Andes of South America and of southern Central America, located  
149 between the continuous forest line and the permanent snowline at about 3000–5000 m (Luteyn, 1999). The grass páramo is  
150 formed by tussock grasses, mainly *Calamagrostis* and *Festuca*. These are complemented by shrubs of *Diplostegium*,  
151 *Hypericum*, and *Pentacalia*, and forest patches of *Polylepis*. The shrub páramo consists of cushion plants like *Azorella*,  
152 *Plantago*, and *Werneria*, and shrubs like *Loricaria* and *Chuquiraga*. The vegetation of the desert páramo is scarce. Some  
153 common taxa are *Nototriche*, *Draba*, and *Culcitium* (Sklenar and Jørgensen, 1999).

154 Ríncon-Martínez et al. (2010) showed that the terrigenous sediment supply at ODP Site 1239 during Pleistocene interglacials  
155 is mainly fluvial and input of terrestrial material drops to low amounts during the drier glacial stages. Consequently, transport  
156 of pollen and spores to the ocean is also mainly fluvial (González et al., 2010). High rates of orographic precipitation  
157 characterize the western part of equatorial South America. These heavy rains quickly wash out any pollen that might be in the  
158 air and result in large discharge by the Ecuadorian Rivers (Fig. 2). Esmeraldas and Santiago Rivers mainly drain the northern  
159 coastal plain of Ecuador, and the southern coastal plain is drained by several smaller rivers, which end in the Guayas River  
160 (Balslev, 1988). Moreover, the predominantly westerly winds (Fig. 2) are not favorable for eolian pollen dispersal to the ocean.  
161 Nevertheless, some transport by SE trade winds is possible and should be taken into account.

162 After reaching the ocean, pollen and spores might pass the Peru-Chile Trench – which is quite narrow along the Carnegie  
163 Ridge – by means of nepheloid layers at subsurface depths. Some northward transport from the Bay of Guayaquil by the  
164 Coastal Current (Fig. 2) is likely. However, the Peru-Chile Current flows too far from the coast to have strong influence on  
165 pollen and spore dispersal. We consider western Ecuador, northernmost Peru and southwestern Colombia the main source  
166 areas of pollen and spores in sediments of ODP Site 1239.

### 167 1.1.3 Drilling site

168 ODP Site 1239 is located at 0°40.32'S, 82°4.86'W, about 120 km offshore Ecuador in a water depth of 1414m, near the eastern  
169 crest of Carnegie Ridge and just next to a downward slope into the Peru-Chile Trench (Mix et al., 2003). Its location is close  
170 to the Equatorial Front (Fig. 2) which separates the warm and low-salinity waters of Panama Basin from the cooler and high-  
171 salinity surface waters of the EEP CT. The region of Site 1239 reveals a thick sediment cover, with dominant sediments in the  
172 region being foraminifer-bearing diatom nannofossil ooze (Mix et al., 2003). A tectonic backtrack path on the Nazca plate  
173 (Pisias, 1995) reveals a paleoposition of Site 1239 about 150–200 km further westward (away from the continent) and slightly  
174 southward relative to South America at 4–5 Ma compared to the present day position (Mix et al., 2003). ~~The sediments of~~  
175 ~~Carnegie Ridge are characterized by high smectite values.~~ Due to its proximity to the Ecuadorian coast, Site 1239 is suitable  
176 to record changes in fluvial runoff, related to variations of precipitation in northwestern South America. Most of the material  
177 is discharged by the Guayas River and Esmeraldas River (Rincon-Martinez et al., 2010).

178

180 **Table 1. List of identified pollen and spore taxa in marine ODP Holes 1239A (Pliocene samples) and 1239B (core top**  
 181 **samples, taxa in grey occurred only in core top samples) and grouping according to their main ecological affinity**  
 182 **(Flantua et al., 2014; Marchant et al., 2002).**  
 183

<b>Páramo</b>	<b>Upper montane forest</b>	<b>Lower montane forest</b>	<b>Lowland rainforest</b>	<b>Broad range taxa</b>	<b>Humid indicators</b>
<i>Polylepis/Acaena</i>	Podocarpaceae	Urticaceae/ Moraceae	<i>Wettinia</i>	Poaceae	Cyperaceae
<i>Jamesonia/Eriosorus</i>	<i>Hedyosmum</i>	<i>Erythrina</i>	<i>Socratea</i>	Cyperaceae	<i>Ranunculus</i>
<i>Huperzia</i>	<i>Clethra</i>	<i>Alchornea</i>	Polypodiaceae	Tubuliflorae (Asteraceae)	<i>Hedyosmum</i>
<i>Ranunculus</i>	<i>Morella</i>	<i>Styloceras T</i>	<i>Pityrogramma/ Pteris altissima T</i>	Amaranthaceae	<i>Ilex</i>
<i>Draba</i>	Acanthaceae	Malpighiaceae		Rosaceae	<i>Pachira</i>
<i>Sisyrinchium</i>	Melastomataceae	Cyatheaceae		<i>Ambrosia/ Xanthium</i>	<i>Morella</i>
<i>Cystopteris diaphana T</i>	<i>Daphnopsis</i>	<i>Vernonia T</i>		Ericaceae	Malpighiaceae
	<i>Bocconia</i>	<i>Pteris grandifolia T</i>		<i>Artemisia</i>	Cyatheaceae
	<i>Myrsine</i>	<i>Pteris podophylla T</i>		<i>Ilex</i>	<i>Selaginella</i>
	<i>Lophosoria</i>	<i>Saccoloma elegans T</i>		<i>Thevetia</i>	<i>Pityrogramma/ Pteris altissima T</i>
	<i>Elaphoglossum</i>	<i>Thelypteris</i>		<i>Salacia</i>	<i>Hymenophyllum T</i>
	<i>Hypolepis hostilis T</i>	<i>Ctenitis subincisa T</i>		Bromeliaceae	<i>Thelypteris</i>
	<i>Grammitis</i>			Malvaceae	<i>Ctenitis subincisa T</i>
	<i>Dodonaea viscosa</i>			Euphorbiaceae	<i>Alnus</i>
	<i>Alnus</i>			<i>Liliaceae</i>	<i>Cystopteris diaphana T</i>
				Lycopodiaceae excl. <i>Huperzia</i> <i>Selaginella</i>	
				<i>Hymenophyllum T</i>	
				<i>Calandrinia</i>	

184

185

## 186 2 Methods

187 A total of 65 samples of 10 cm<sup>3</sup> volume have been analyzed. For the interval between 301 and 334 mbsf (4.7 and 4.2 Ma), 46  
 188 sediment samples were taken at 67 cm intervals on average from ODP Hole 1239A (cores 33X5-37X1). Seventeen samples  
 189 were taken more or less regularly distributed over the rest of the upper 450 m of Hole A (until 6 Ma). Additionally, two core  
 190 top samples were taken from ODP Hole 1239B as modern analogues. Standard analytical methods were used to process the  
 191 samples, including decalcification with HCl (~10%) and removal of silicates with HF (~40%). Two tablets of exotic  
 192 *Lycopodium* spores (batch #177,745 containing 18584 ± 829 spores per tablet) were added to the samples during the  
 193 decalcification step for calculation of pollen concentrations (grains/cm<sup>3</sup>). After neutralization with KOH (40%) and washing,  
 194 the samples were sieved with ultrasound over an 8µm screen to remove smaller particles. Samples were mounted in glycerin

195 and a minimum of 100 pollen/spore grains (178 on average, [Supplementary Figure Fig. S1](#)) were counted in each sample using  
196 a Zeiss Axioskop and 400x and 1000x (oil immersion) magnification.

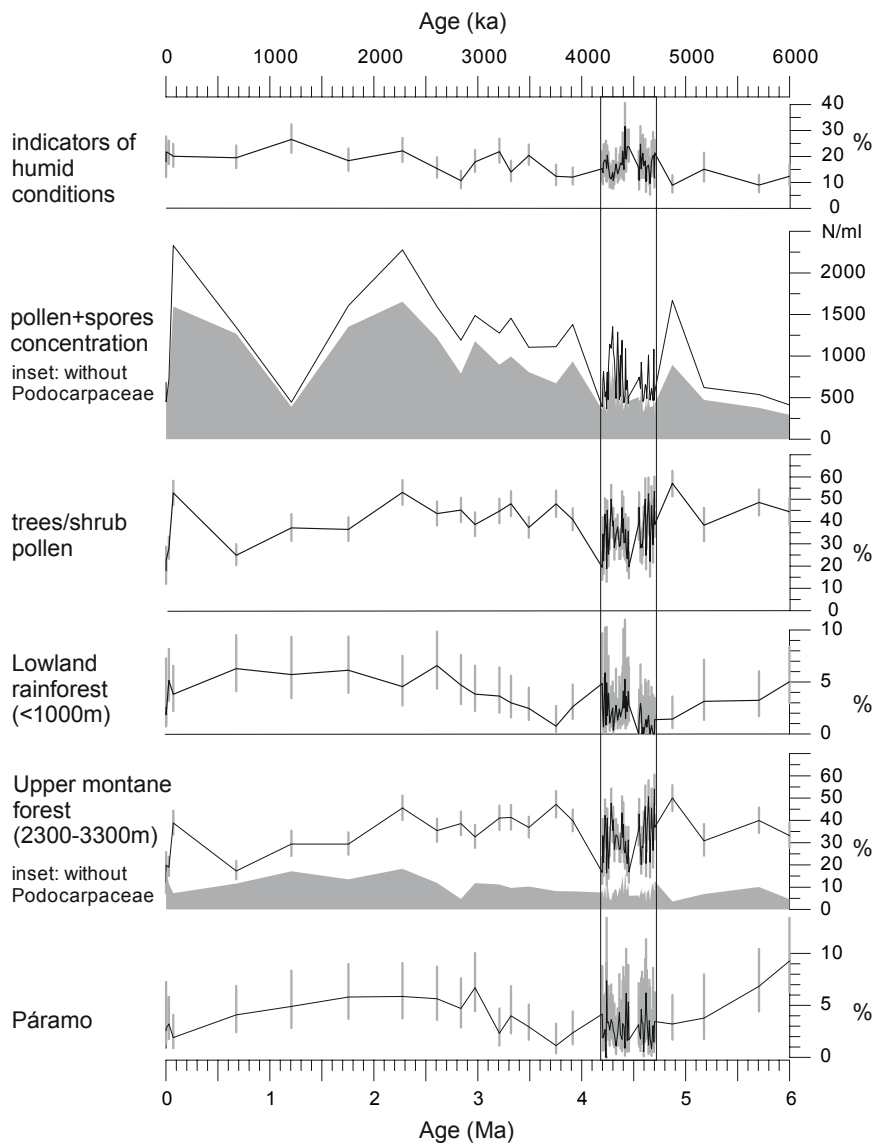
197 For pollen identification, the Neotropical Pollen Database (Bush and Weng, 2007), a reference collection for Neotropical  
198 species held at the Department of Palynology and Climate Dynamics in Göttingen, and related literature (Colinvaux et al.,  
199 1999; Hooghiemstra, 1984; Murillo and Bless, 1974, 1978; Roubik and Moreno, 1991) were used. Pollen types were grouped  
200 according to their main ecological affinity (Flantua et al., 2014; Marchant et al., 2002). The zonation of the diagrams was  
201 based on constrained cluster analysis by sum-of-squares (CONISS) of the pollen percentage curves, using the square root  
202 transformation method (Edwards & Cavalli-Sforza's chord distance) implemented in TILIA (Grimm, 1991, [Supplementary](#)  
203 [Figure](#)). Percentages are based on the pollen sum, which includes all pollen and fern spore types including unidentifiable ones.  
204 Confidence intervals were calculated after Maher (1972). An initial age model for Site 1239 was established based on  
205 biostratigraphic information (Mix et al., 2003). The age model was refined by matching the benthic stable isotope records from  
206 Site 1239 with those from Site 1241 by visual identification of isotope stages (Tiedemann et al., 2007). [Site 1241 has an](#)  
207 [orbitally tuned age model. Thus, this procedure resulted in an indirectly orbitally tuned age model for Site 1239, spanning](#)  
208 [the interval from 5 to 2.7 Ma \(Tiedemann et al., 2007, Fig. S2\). A coring gap of ca. 5 meters exists between cores 35X \(347](#)  
209 [mcd\) and 36X \(352 mcd\) of Hole 1239A \(Tiedemann et al., 2007; Table AT3\).](#)

210 Elemental concentrations (total elemental counts) of Fe and K were measured in high resolution (every 2 cm) using an  
211 Avaatech™ X-Ray Fluorescence (XRF) Core Scanner at the Alfred-Wegener-Institute, Bremerhaven, [with correction for dead](#)  
212 [time](#). Both Holes A and B of ODP Site 1239 were sampled. A nondestructive measuring technique was applied, allowing rapid  
213 semi-quantitative geochemical analysis of sediment cores (Richter et al., 2006). Several studies comparing XRF core scanner  
214 data to geochemical measurements on discrete samples showed that major elements ~~such as Fe, Ca, and K~~ can be precisely  
215 measured with the scanner in a non-destructive way (e.g. Tjallingii et al., 2007).

### 216 **3 Results**

217 Five groups were established with pollen taxa grouped according to their main ecological affinity (Table 1). The groups  
218 páramo, upper montane forest, lower montane forest, and lowland rainforest represent vegetation belts with different altitudinal  
219 ranges (Hooghiemstra, 1984; Van der Hammen, 1974). To track changes of humidity, an additional group named “Indicators  
220 of humid conditions” was established. This group includes those taxa that permanently need humid conditions to grow.  
221 Changes of the pollen percentages of the ecological groups for the Pliocene interval and the core top samples are shown in  
222 [Figs. 3 and 5. Pollen percentages of single taxa are shown in \[the Supplementary Figure Fig. S1\]\(#\).](#)

223 To put the results of the detailed early Pliocene section into context of long-term changes, we plot a selection together with  
224 the results of a coarse resolution pilot study in Fig. 3. Percentages of humidity indicators hint to slightly drier conditions at the  
225 beginning of the Pliocene. A trend towards higher palynomorph concentrations is found for the period from 6 to 2 Ma. Grass  
226 pollen percentages remain low indicating mainly closed forest at altitudes below the páramo. Representation of lowland  
227 rainforest was low around 4.7 Ma, increased by 4.5 Ma, declined again to low levels around 3.5 Ma, and rose to remain at  
228 higher levels during the Pleistocene. Continuous presence of pollen and spores from the páramo indicates that the Ecuadorian  
229 Andes had reached high altitudes before the Pliocene.

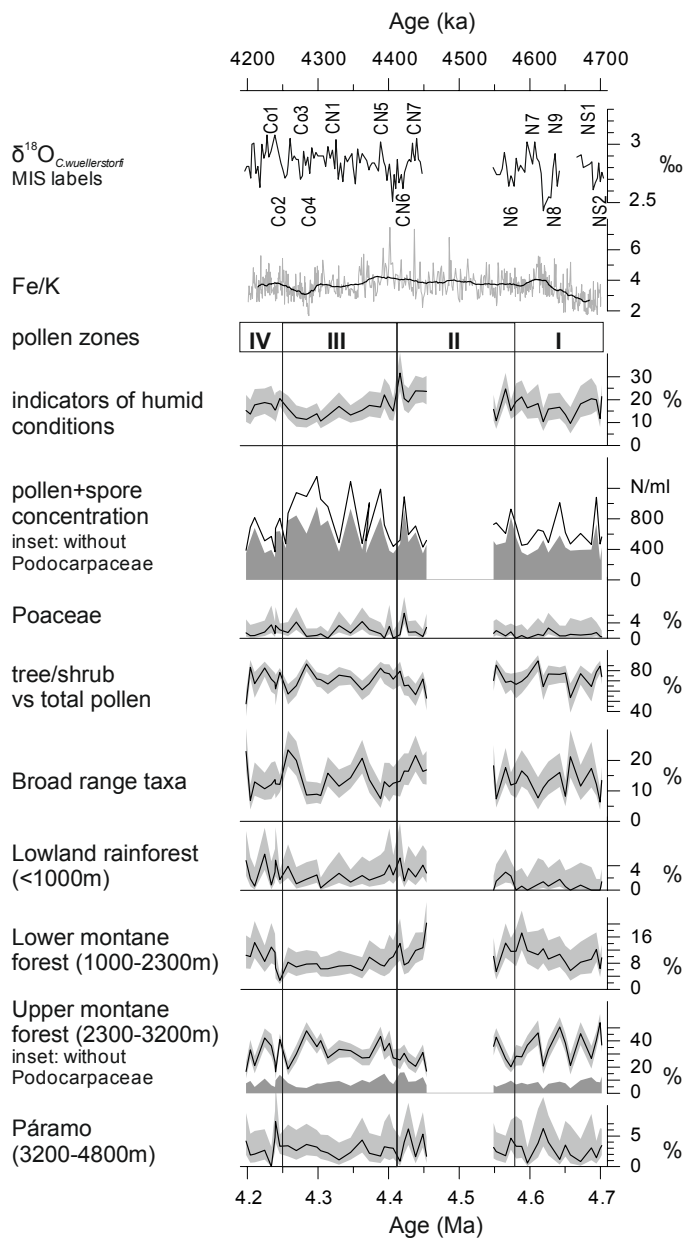


231

232 **Figure 3. Pliocene and Pleistocene palynomorph percentages (based on the total of pollen and spores) of ODP Hole 1239A for three**  
 233 **vegetation belts, humidity indicators, grass pollen and pollen and spore concentration per ml. 95% confidence intervals as grey bars**  
 234 **after Maher (1972). Age model for the last 5 Ma after Tiedemann et al. (2007) and for 6 to 5 Ma after Mix et al. (2003).**

### 235 3.1 Description of the early Pliocene pollen record

236 In the early Pliocene samples, 141 different palynomorph types were recognized, including 77 pollen and 64 fern spore types.  
 237 A high percentage of tree and shrub pollen (46–88%) is present throughout the interval, compared to low percentages of herbs  
 238 and grass pollen (0–25%; Fig. 4). In most of the vegetation belts, one or two pollen or spore taxa are overrepresented. The  
 239 lowland rainforest is mainly represented by Polypodiaceae, the lower montane forest is controlled by Cyatheaceae, and the  
 240 upper montane forest is strongly influenced by Podocarpaceae and *Hedyosmum*. In the páramo, the percentages of the pollen  
 241 taxa are more evenly balanced. Of the total sum, the Andean forest pollen makes by far the largest percentage, with the upper  
 242 montane forest ranging between 17 and 54% and the lower montane forest between 5 and 19%. The páramo is represented  
 243 with 0 to 10% and the lowland rainforest with 0 to 6%. The remaining fraction has a wide or unknown ecological range.  
 244



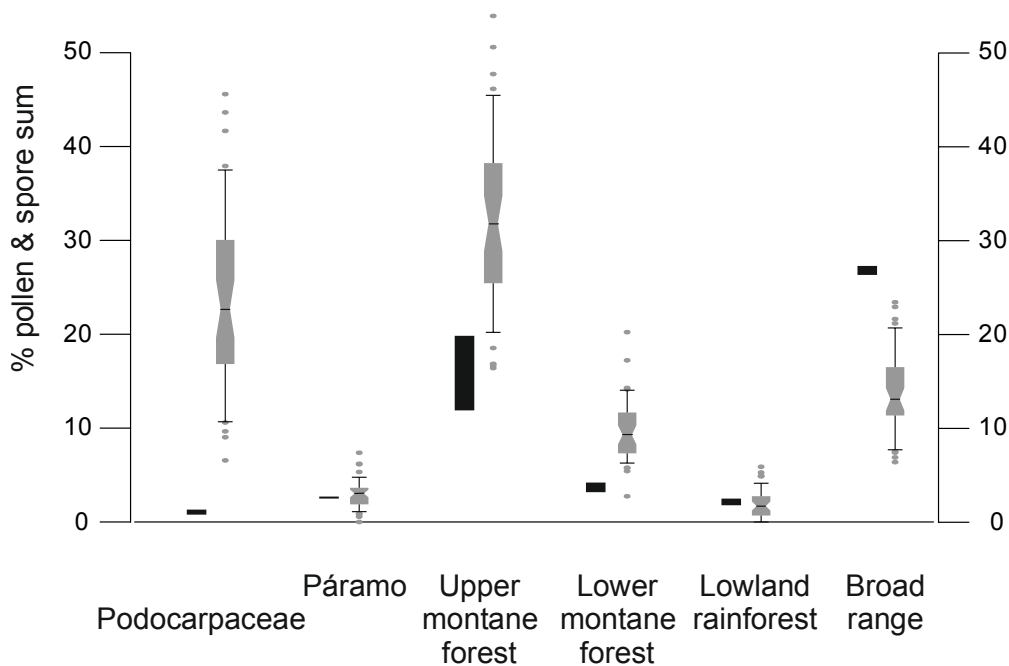
245

246 **Figure 4. Palynomorph percentages of ODP Hole 1239A for the four vegetation belts and other groups from 4.7 to 4.2 Ma. Grey**  
 247 **shading represents the 95% confidence intervals (after Maher, 1972). Vertical black lines delimit the pollen zones. At the top stable**  
 248 **oxygen isotopes of the benthic foraminifer *C. wuellerstorfi* (Tiedemann et al., 2007) of ODP Hole 1239A, marine isotope stages (MIS),**  
 249 **and elemental ratios of Fe/K from Holes 1239A and 1239B. Ages are from Tiedemann et al. (2007). A coring gap is present in Hole**  
 250 **1239A between 4.45 and 4.55 Ma.**

251

252 The pollen record of ODP Hole 1239A was divided into four main pollen zones based on constrained cluster analysis (Fig. 4  
 253 and [Supplementary Figure Fig. S1](#)). Pollen zone I (333.4–325.2 mbsf: 4.70–4.58 Ma, 14 samples) has low pollen and spores  
 254 concentrations. It is characterized by low pollen percentages of lowland rainforest, increases in pollen values of lower montane  
 255 forest, the percentage of fern spores, and the Fe/K ratio. The pollen concentrations of broad range taxa, upper montane forest,  
 256 páramo, and indicators of humid conditions go through frequent fluctuations. Coastal desert herbs (Amaranthaceae) are well  
 257 represented ([Supplementary Figure Fig. S1](#)). Percentages of Poaceae pollen are low. In pollen zone II (324.8–316.4 mbsf: 4.46–  
 258 4.42 Ma, 10 samples), the pollen and spores concentration is similar to pollen zone I. The lowland rainforest pollen, indicators  
 259 of humid conditions, and the Fe/K ratio reach their maximum. Fern spores also reach their first maximum. Percentages of  
 260 lower montane forest and páramo are high, whereas the percentage of upper montane forest is low at this time due to a strong  
 261 decline of Podocarpaceae pollen. The representation of broad range taxa diminish in the interval above the gap, the decrease  
 262 being mainly controlled by *Selaginella*, *Cyperaceae*, *Ambrosia/Xanthium*, and *Amaranthaceae*. Pollen zone II encloses a coring  
 263 gap of almost 100 ka. Pollen zone III (315.5–305.4 mbsf: 4.41–4.26 Ma, 14 samples) shows a stepwise increase of the pollen

264 and spores concentration with its maximum at 4.3 Ma. The concentration is strongly controlled by Podocarpaceae pollen which  
 265 account for up to 44% in this zone. The pollen of lowland rainforest, lower montane forest, páramo, indicators of humid  
 266 conditions, and Fe/K show lower values than in zone II. Broad range taxa show some larger fluctuations. The upper montane  
 267 forest pollen has its maximum extent of this zone (48%) at 4.28 Ma due to the high percentage of Podocarpaceae. If the  
 268 Podocarpaceae pollen are excluded from the upper montane forest, the representation of this vegetation belt shows the same  
 269 pattern of decline as that of the lower montane forest and lowland rainforest. In pollen zone IV (304.7–301.3 mbsf: 4.25–4.12  
 270 Ma, 8 samples), the pollen and spores concentration decreases sharply after 4.24 Ma. The pollen percentage of lower montane  
 271 forest increases. The percentage of fern spores is at its maximum in this zone. Percentages of páramo, upper montane forest,  
 272 broad range taxa, indicators of humid conditions, and the Fe/K ratio remain similar as in zone III. The percentage of lowland  
 273 rainforest pollen goes through frequent and large fluctuations.



274  
 275 **Figure 5. Comparison of the palynomorph percentages (based on total pollen and spores) of Podocarpaceae and the different**  
 276 **vegetation belts between 2 Holocene samples (black) and Pliocene samples between 4.7–4.2 Ma (box-whisker plots).**

277

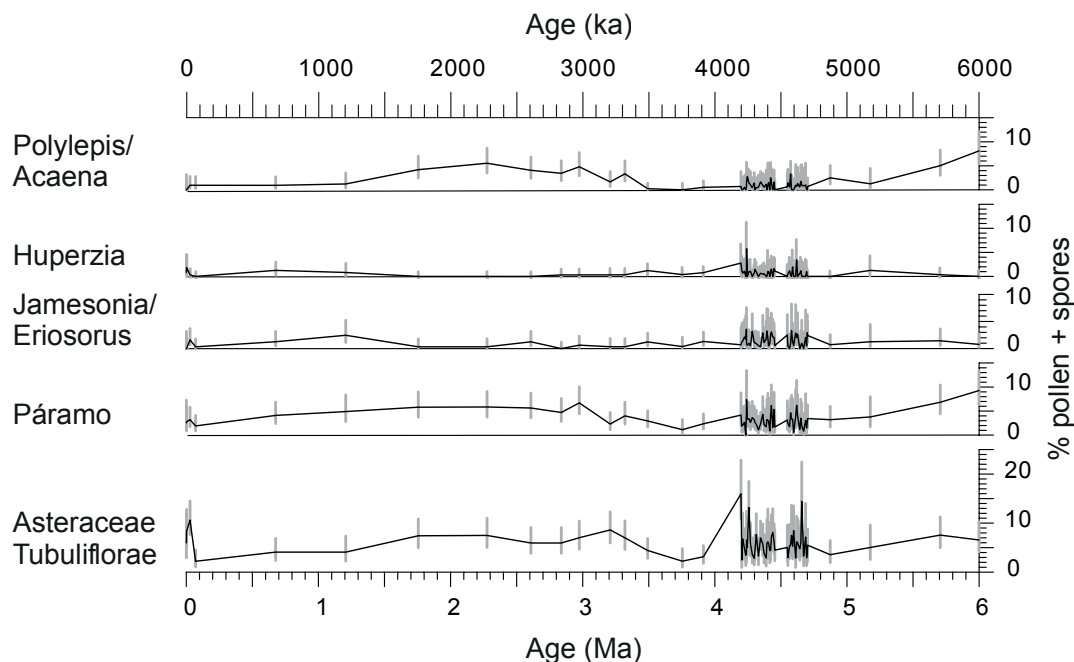
### 278 3.2 Modern vs. Pliocene pollen assemblages

279 Two samples from the top of ODP Hole 1239B have been analyzed to facilitate a comparison of the recent palynological signal  
 280 with modern vegetation (Fig. 5 and [Supplementary Figure Fig. S1](#)). Although there is no detailed age control on these  
 281 surface/subsurface samples, a Holocene age can be assigned based on the benthic oxygen isotope record (Rincon-Martinez et  
 282 al., 2010). Fifty-one different palynomorph types were recognized, including 29 pollen and 22 fern spore types. The samples  
 283 are characterized by low pollen and spore concentrations of 685 and 465 grains/cm<sup>3</sup>, respectively. Indicators of humid  
 284 conditions show intermediate values. Herbs and grass pollen are very abundant with 20–26%, but tree and shrub pollen  
 285 decreased to 35–46% compared to the early Pliocene interval. Broad range taxa reach their maximum abundance with 26–  
 286 27%. Lowland rainforest and páramo pollen have similar representations as in the Pliocene, whereas the lower and upper  
 287 montane forest pollen reach their lowest percentages. When compared to the Pliocene pollen composition, some floristic  
 288 differences are seen. During the Holocene *Podocarpus* is replaced by *Alnus* as the most abundant upper montane forest tree,  
 289 although *Podocarpus* was still abundant during the glacial (González et al. 2010). Another notable difference is the presence  
 290 of *Rhizophora* pollen in one of the core top samples, whereas it is completely absent in the early Pliocene interval.



291 **3.3 Description of the páramo**

292 The pollen spectrum from the páramo at ODP Site 1239 includes three different taxa which are mainly confined to the páramo:  
293 the pollen type *Polylepis/Acaena*, and the fern spores *Huperzia* and *Jamesonia/Eriosorus* (Fig. 6). Other taxa, which are  
294 characteristic of páramos but cannot be exclusively attributed to this ecosystem, were not included in the páramo sum (e.g.  
295 Asteraceae, Poaceae, Ericaceae). The record shows the continuous presence of páramo vegetation since at least 6 Ma. The  
296 summed páramo pollen constitutes up to 9% of the total pollen and spore sum, with the highest fraction found at the beginning  
297 of the record (6 Ma), and the lowest fractions around 4.23 and 4.59 Ma, at ca. 3.75 Ma and during the late Pleistocene (Figs.  
298 4 and 6).  
299



300  
301 **Figure 6. Palynomorph percentages of páramo indicators and Asteraceae Tubuliflorae (excluding *Ambrosia/Xanthium* T) of the past**  
302 **6 Ma indicating the presence of páramo vegetation at least since the late Miocene. 95% confidence intervals (grey bars) after Maher**  
303 **(1972). Ages after Tiedemann et al. (2007) and Mix et al (2003).**

304

305 **4 Discussion**

306 **4.1 Fe/K as a tracer for changes in fluvial runoff**

307 The Fe/K ratio has been shown to be a suitable tracer to distinguish between terrigenous input of slightly weathered material  
308 from drier regions and highly weathered material from humid tropical latitudes. Sediments from deeply chemically weathered  
309 terrains have higher iron concentrations compared to the more mobile potassium (Mulitza et al., 2008). Before paleoclimatic  
310 interpretations can be made based on elemental ratios, other processes which possibly influence the distribution of Fe/K in  
311 marine sediments should be examined, like changes of the topography of Andean river drainage basins, the input of mafic rock  
312 material, or diagenetic Fe remobilization (Govin et al., 2012). For northeastern South America it was shown that during the  
313 middle Miocene, uplift of the Eastern Andean Cordillera led to changes in the drainage direction of the Orinoco and Magdalena  
314 rivers and to the formation of the Amazon River (Hoorn, 1995; Hoorn et al., 2010). If a similar temporal history of uplift and  
315 changing drainage patterns is assumed for the western Andean Cordillera, the large-scale patterns of the present topography  
316 and river drainage basins should have been in place by the early Pliocene. Therefore, the main direction of fluvial transport of  
317 Fe should have been similar to today. Diagenetic alteration was shown not to affect Fe concentrations at Site 1239 (Rincon-  
318 Martinez, 2013). The Fe/K ratio therefore seems to be an adequate tracer of fluvial input at this study site. The trend of Fe/K

319 is similar to the pattern of humidity inferred from the pollen spectrum, showing the highest values around 4.46 Ma, thus  
320 supporting the hydrological interpretation of the pollen record.

## 321 **4.2 The Holocene as modern reference**

322 In order to better understand the source areas and transport ways of pollen grains to the sediments, we make a comparison of  
323 the results of our two Holocene samples ([Supplementary Figure Fig. S1](#)) with that of another pollen record retrieved from the  
324 Carnegie Ridge southeast of ODP Site 1239 (TR 163-38, Fig. 2) reflecting rainfall and humidity variation of the late Pleistocene  
325 (González et al. 2006). Holocene samples of Site 1239 gave similar results showing extensive open vegetation (indicated by  
326 pollen of Poaceae, Cyperaceae, Asteraceae) and maximum relative abundance of fern spores although concentration is low  
327 (González et al., 2006). As also indicated by the elemental ratios, fluvial transport of pollen predominates in this area (González  
328 et al., 2006; Ríncón-Martínez, 2013). This is understandable, as both ocean currents and wind field do not favor transport from  
329 Ecuador to Site 1239 (Fig. 2).

330 Despite the expansion of open vegetation, González et al. (2006) interpreted this record to reflect permanently humid  
331 conditions, with disturbance processes caused by human occupation and more intense fluvial dynamics. The relatively high  
332 percentage of indicators of humid conditions in our core top samples compared to pollen zones III and IV in the early Pliocene  
333 would be in agreement with this interpretation. The core top samples from ODP hole 1239B and the most recent part of core  
334 TR 163-38 are taken as a basis for the hydrological interpretation of the Pliocene pollen record.

## 335 **4.3 Climatic implications of vegetation change**

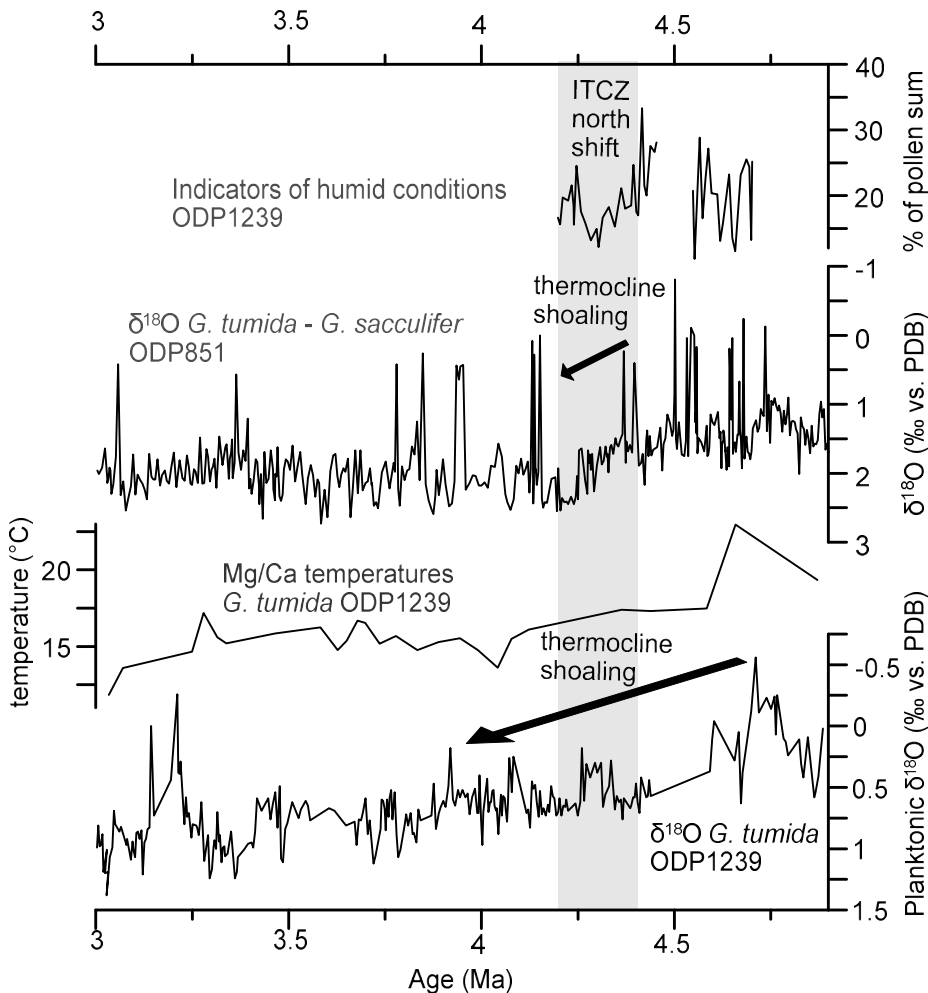
336 The presented marine palynological record provides new information on floristic and vegetation changes occurring along  
337 diverse ecological and climatic gradients through the early Pliocene. The consistently high percentage of tree and shrub pollen,  
338 compared to a low percentage of herbs and grass pollen (< 25%) suggests the predominance of forests and the nearly absence  
339 of open grasslands (apart from páramo) during the early Pliocene. Moreover, the very low percentage of dry indicators  
340 (Amaranthaceae) suggests the absence of persisting drought conditions and supports the idea of a rather stable and humid  
341 climate that favored a closed forest cover. This is in good accordance with Pliocene climate models suggesting warmer and  
342 wetter conditions on most continents, which led to expansions of tropical forests and savannas at the expense of deserts, for  
343 instance in Africa (Salzmann et al., 2011). During the early Pliocene, no profound changes in the vegetation occur. All  
344 altitudinal vegetation belts are already present, with varying ratios, and only pollen percentages of lowland rainforest rise from  
345 almost absent to 6%.

346 Shifts in the vegetation are driven by various parameters such as temperature, precipitation, CO<sub>2</sub>, radiation, and any  
347 combination thereof. However, a hint to which parameter has strongest influence on the vegetation might be given by the  
348 pattern of expansion and retreat of different vegetation belts. Hooghiemstra and Ran (1994) indicate that if temperature were  
349 the dominant driver of vegetation change, altitudinal shifting of vegetation belts would lead to increase in the representation  
350 of one at the cost of another. We hardly see such a pattern in our record with the possible exception in zone III where the trends  
351 between pollen percentages of páramo and those of upper montane forest (without Podocarpaceae) are reversed (Section 4.3.2;  
352 Fig. 8). However, the more general pattern indicates parallel changes in the representation of the forest belts suggesting that  
353 not temperature but humidity had the stronger effect on the Pliocene vegetation of Ecuador.

### 354 **4.3.1 Development of the coastal vegetation**

355 Early Pliocene pollen zones I and IV show an expansion of coastal desert herbs (Amaranthaceae, [Supplementary Figure Fig.](#)  
356 [S1](#)), which coincides with low sea-surface temperatures at ODP Site 846 in the EEP, suggesting an influence of the Peru-Chile  
357 Current (continuation of the Humboldt Current) on the coastal vegetation of southern Ecuador. Remarkably, the lowland  
358 rainforest and the coastal desert herbs follow a similar trend. This seems odd at the first glance, but a possible mechanism to

359 explain this pattern would invoke effects of El Niño, the warm phase of ENSO. The main transport agent for pollen in this  
 360 region are rivers, but in the coastal desert area of southern Ecuador and northern Peru, fluvial discharge rates are low (Milliman  
 361 and Farnsworth, 2011). Therefore, pollen might be retained on land until an El Niño event causes severe flooding in the coastal  
 362 areas (Rodbell et al., 1999) and episodically fills the rivers which transport the pollen to the ocean. Such possible effects of El  
 363 Niño seem to be strongest in pollen zones I and IV where pollen percentages of the lowland rainforest and coastal desert herbs,  
 364 but also the upper montane forest, fluctuate most strongly. The lowland rainforest of the coastal plain of Ecuador and western  
 365 Colombia is within the present-day range of the ITCZ, and expanded from 4.7 Ma onwards possibly due to a southwards  
 366 displacement of the mean latitude of the ITCZ (Figs. 3 and 4).  
 367



368  
 369 **Figure 7.** Percentages of indicators of humid conditions (ODP Site 1239, this study), *G. tumida* – *G. sacculifer* difference in  $\delta^{18}\text{O}$  from  
 370 ODP Site 851 in the eastern equatorial Pacific (Cannariato and Ravelo, 1997), and *G. tumida* Mg/Ca temperatures and  $\delta^{18}\text{O}$  from  
 371 ODP Site 1239 (Steph, 2005; Steph et al., 2010). Grey shading marks the period of thermocline shoaling at ODP Site 851 and ITCZ  
 372 north shift.

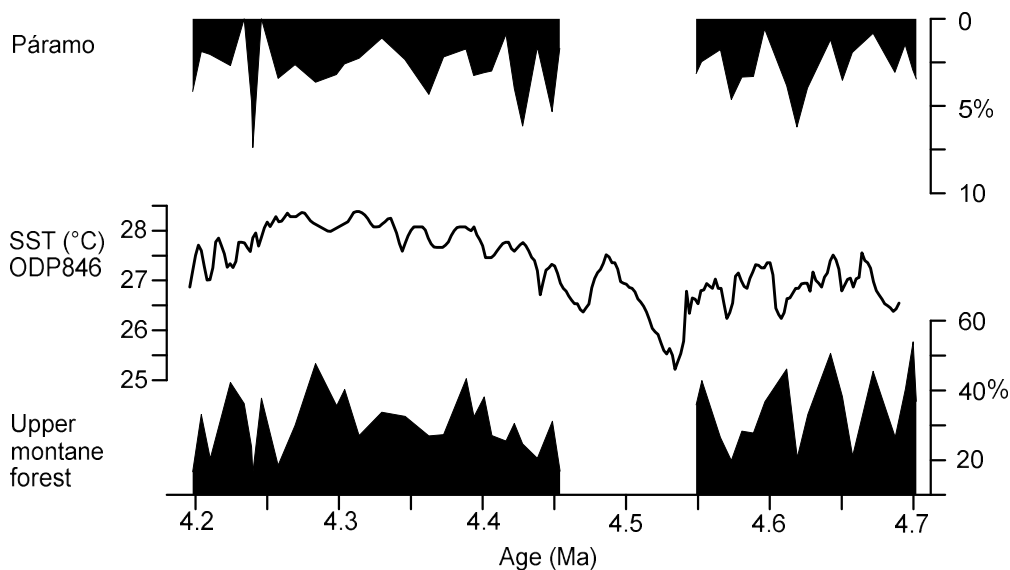
373  
 374 **4.3.2 Development of the montane vegetation**

375 Podocarpaceae strongly dominate the pollen spectrum in general. However, the trend in pollen percentages of Podocarpaceae  
 376 divert from that of the other pollen taxa, which may be explained by additional transport of Podocarpaceae pollen by wind.  
 377 The high pollen production of Podocarpaceae and their specialized morphology (Regal, 1982) facilitate their eolian transport.  
 378 In contrast, pollen from most other taxa is predominantly fluvially transported (González et al., 2006), therefore exhibiting a  
 379 different pattern where high pollen concentrations correspond to high fluvial discharge in the source area. Eolian transport of  
 380 Podocarpaceae explains the high pollen concentrations in pollen zone III, which occur despite less humid conditions compared

381 to pollen zones II and IV. The increased eolian transport at 4.63 Ma and between 4.4 and 4.25 Ma is proposed here to be the  
 382 result of an intensification of the easterly trade winds. Increase in trade wind strength at 4.4 Ma would be in line with a shift  
 383 in the locus of maximum opal accumulation rates in the ocean associated with a shift in nutrient availability from ODP Site  
 384 850 to ODP Site 846 nearer to the continent (positions shown in Fig. 2) (Farrell et al., 1995). Dynamic modelling indicates  
 385 that stronger easterlies would cause shoaling of the EEP thermocline (Zhang et al., 2012), which took place between 4.8 and  
 386 4.0 Ma (Fig. 7; Steph et al., 2006a). Related to this process, a critical step of easterly trade wind intensification, indicated by  
 387 increased eolian transport of Podocarpaceae pollen, occurred between 4.4 and 4.25 Ma.

388 Comparing the pollen percentages of páramo and upper montane forest, (Fig. 8) indicates that UMF maxima coincide with  
 389 páramo minima and SST maxima at ODP Site 846 (Lawrence et al., 2006). This might be explained by a shift of the upper  
 390 montane forest to higher altitudes at the cost of the area occupied by páramo vegetation as a result of higher atmospheric  
 391 temperatures and/or increased orographic precipitation in the western Andean Cordillera caused by higher sea-surface  
 392 temperatures and increased evaporation.

393



394

395 **Figure 8. Pollen percentages of upper montane forest and páramo, and UK'37 sea-surface temperatures (SST) of ODP site 846 in**  
 396 **the eastern equatorial Pacific (Lawrence et al., 2006).**

397

#### 398 4.4 Development of the páramo and implications for Andean uplift

399 In order to use the existence of páramo vegetation as an indicator for Andean elevation, the altitudinal restriction of the páramo  
 400 taxa to environments above the forest line is a prerequisite. Although no taxa restricted to páramo were identified in the marine  
 401 samples, or rather, they could not be identified due to the lack of genus-level morphological distinction (especially *Espeletia*  
 402 from the Asteraceae and some Poaceae, e.g. *Festuca*), several taxa are mainly confined to high Andean environments. Dwarf  
 403 trees of *Polylepis* typically form patches above the forest line and its natural altitudinal range is thought to occur between a  
 404 lower limit which forms the transition to other forest types and up to 5000 m in Bolivia (Kessler, 2002). *Huperzia* occurs in  
 405 montane forests as epiphytes and with terrestrial growth form in the páramo (Sklenar et al., 2011). *Jamesonia* and *Eriosorus*  
 406 are both found in cool and wet highlands, with most species being found between 2200 and 5000 m (Sánchez-Baracaldo,  
 407 2004). Asteraceae are not restricted to the páramo, but their occurrence in the montane forest and in the lowland rainforest of  
 408 the Pacific coast is scarce (Behling et al., 1998). With a contribution of up to 16% of the pollen sum, their source area can be  
 409 attributed mainly to the páramo. Additionally, the fluctuations are similar to the other páramo taxa (Fig. 6), which is another  
 410 indication for their common source area.

411 The pollen record shows a continuous existence of páramo vegetation. During the warm Pliocene, the upper montane forest is  
412 assumed to have extended to similar or even higher altitudes as today. Despite this upward expansion of the upper montane  
413 forest, the páramo was still present, which implies that the western Cordillera of the Ecuadorian Andes had already gone  
414 through substantial uplift by that time. Furthermore, the pollen record has a large montane signature, which would not be the  
415 case if the Andes had reached less than half of their modern height by the early Pliocene (Coltorti and Ollier, 2000). The upper  
416 montane forest which constitutes up to 60% of the pollen sum shows that montane habitats with the corresponding altitudinal  
417 belts were already existent. These findings suggest an earlier development of the high Andean páramo ecosystem than  
418 previously inferred from palynological studies of the eastern Cordillera in Colombia (Hooghiemstra et al., 2006; Van der  
419 Hammen et al., 1973). This might also be an indication that the uplift history of the western Cordillera of Ecuador is temporally  
420 more closely related to the uplift of the Central Andes where a major phase of uplift occurred between 10 and 6 Ma (Garziona  
421 et al., 2008). In another recent palynological study, the arrival of palynomorphs from the páramo in sediments of the Amazon  
422 Fan has been documented since 5.4 Ma (Hoorn et al., 2017). Since the Amazon has its westernmost source in Peru, this signal  
423 might be related to the uplift of the Central Andes. These new records agree with paleoclimatic studies showing that modern  
424 type precipitation patterns have likely been in place since the middle Miocene (Barnes et al., 2012; Hoorn et al., 2010;  
425 Kaandorp et al., 2006), which would have required a significant orographic barrier. High Andean mountains acting as a climate  
426 divide might thus go as far back as the Mid-Miocene. However, earliest evidence for a páramo vegetation is now set at latest  
427 Miocene.

#### 428 **4.5 Comparing models and proxy data**

429 Several studies have suggested the existence of a “permanent El Niño” during the Pliocene (e.g. Fedorov et al., 2006; Wara et  
430 al., 2005). El Niño events are characterized by a shift in the Walker circulation, resulting in exceptionally heavy precipitation  
431 particularly over the lowlands of central and southern Ecuador (Bendix and Bendix, 2006) and simultaneous below-average  
432 rainfall over the northwestern slopes of the Andes (Vuille et al., 2000). A permanent El Niño-like climate state during the early  
433 Pliocene would thus have involved permanently humid conditions with high rates of precipitation and fluvial discharge in the  
434 lowlands. Such a climate would have favored the persistence of a broad rain forest coverage and precluded the development  
435 of the desert that exists in coastal southern Ecuador today. The presented pollen record indeed indicates very humid conditions  
436 and the only indicator of dry vegetation is a small percentage of Amaranthaceae pollen. The predicted pattern of expansion of  
437 lowland rainforest at the cost of Andean forest during permanent El Niño is not reflected in the pollen record.

438 The hypothesis of a permanent El Niño climate state involving a reduced zonal Pacific sea-surface temperature gradient has  
439 recently been questioned as sea-surface temperature reconstructions differ substantially depending on the method. Zhang et al.  
440 (2014) claim that a zonal temperature gradient of ca. 3°C existed since the late Miocene and even intensified during the  
441 Pliocene. Our pollen record instead indicates an influence of periodic El Niño-related variations on the coastal and montane  
442 vegetation, especially between 4.7 and 4.55 Ma and between 4.26 and 4.2 Ma, recorded by strong fluctuations in the pollen  
443 percentages of coastal and montane vegetation. Our record does not show increased representation of one vegetation belt at  
444 the cost of another indicating that altitudinal shifts were not extensive and moisture availability might have been an important  
445 driver of Pliocene vegetation change. Changes in humidity could be caused by a latitudinal displacement of the ITCZ. A  
446 southward displacement of the ITCZ over both Atlantic and Pacific has been proposed as a response to stronger zonal  
447 temperature and pressure gradients which developed after the restriction of the Central American Seaway and/or a weakening  
448 of Southern Hemisphere temperature gradients (Billups et al., 1999). The timing of the southward shift was narrowed down to  
449 4.4 to 4.3 Ma in this study, based on  $\delta^{18}\text{O}$  records of planktonic foraminifera. The pollen record suggests a slightly different  
450 timing, with a gradual southwards displacement of the ITCZ between 4.7 Ma and 4.42 Ma when the southernmost position  
451 was reached. A less humid phase, indicated by a decrease of humid indicators, lowland rainforest pollen, lower montane forest  
452 pollen, and the Fe/K ratio, followed between 4.42 and 4.26 Ma where the ITCZ presumably had a slightly more northern

453 position. This phase coincides with the shoaling of the thermocline at ODP Site 851 in the eastern equatorial Pacific  
454 (Cannariato and Ravelo, 1997, Fig. 6). A southward displacement of the ITCZ during the early Pliocene would also be in  
455 accordance with eolian deposition patterns in the EEP which show a latitudinal shift in eolian grain-size and eolian flux  
456 between 6 and 4 Ma (Hovan, 1995). The rather small and slow changes in humidity imply that the ITCZ shift was a gradual  
457 process, rather than the response to a single threshold. Just like the Central American Seaway was restricted and reopened  
458 several times before its definitive closure at around 2.8 Ma (O'Dea et al., 2016), the atmospheric circulation might have adapted  
459 gradually in several small steps to these tectonic changes.

460 Numerical models suggesting a northward shift of the ITCZ in response to the closure of the Central American Seaway or the  
461 uplift of the northern Andes do not necessarily disagree with an early Pliocene southward shift inferred from proxy data. Both  
462 events occurred gradually over several millions of years and despite recent advances in constraining these events, the timing  
463 of major phases in the uplift histories are still debated. In the case of the Central American Seaway, the timing of surface water  
464 restriction based on diverging salinities in the Caribbean and Pacific ocean, respectively, is well constrained and numerous  
465 global oceanographic changes have been associated with it. Possibly these oceanic reorganizations did not directly trigger  
466 modifications of the atmospheric circulation (Kaandorp et al., 2006; Hoorn et al., 2010), but critical periods of uplift  
467 influencing atmospheric circulation might have occurred earlier. On the other hand, the respective model sensitivity  
468 experiments generally only consider isolated changes in single boundary conditions (e.g. closed or open Central American  
469 Seaway). Therefore, the effect of those (i.e. a northward shift of the ITCZ) might counteract the general trend of a southward  
470 shift since the late Miocene due to a decrease in the hemispheric temperature gradient (e.g. Pettke et al., 2002). Additionally,  
471 global coupled models exhibit uncertainties in the representation of ocean-atmosphere feedback and cloud-radiation  
472 feedbacks, which are especially strong in the study region (i.e. showing a double ITCZ and an extensive EEP cold tongue (Li  
473 and Xie, 2014)). This is problematic also in the light of the high sensitivity of the ITCZ position to slight shifts in the  
474 atmospheric energy balance (Schneider et al., 2014). Another aspect to consider is that whereas proxy records record the  
475 transient response of the climate system over a limited period of time, the mentioned model simulations rather follow the  
476 overall equilibrium response than reproducing a stepwise process of environmental changes.

477 Concerning the uplift of the northern Andes, there is still a large uncertainty about the time when the Cordilleras reached their  
478 current elevation. Moreover, phases of major uplift might have strongly differed regionally. Paleobotanists (e.g. Hooghiemstra  
479 et al., 2006; Hoorn et al., 2010; Van der Hammen et al., 1973) and some tectonic geologists (e.g. Mora et al., 2008) argued for  
480 a rapid rise of the Eastern Cordillera since 4–6 Ma, while others conclude that this is rather unlikely implying an earlier uplift  
481 based on biomarker-based paleotemperatures (e.g. Anderson et al., 2015; Mora-Páez et al., 2016). Possibly the Pliocene  
482 oceanic reorganizations did not directly trigger modifications of the atmospheric circulation, which probably was more or less  
483 in place (Kaandorp et al., 2006; Hoorn et al., 2010). Critical periods of uplift influencing atmospheric circulation might have  
484 occurred earlier (see also above). The estimates for uplift of the western Cordillera in Ecuador differ even more strongly, and  
485 range from rapid exhumation around 13 and 9 Ma based on thermochronology (Spikings et al., 2005) to a recent uplift during  
486 the Pliocene and Pleistocene (Coltorti and Ollier, 2000). Our pollen record from the páramo shows that the Ecuadorian Andes  
487 must have already reached close to modern elevations by the early Pliocene in line with inferences of Hoorn et al. (2017) and  
488 Bermúdez et al. (2015). If an early Andean uplift is assumed, the atmospheric response predicted by the model would have  
489 occurred earlier, which would also be in agreement with proxy data indicating a northern position of the ITCZ during the late  
490 Miocene (Hovan, 1995).

491 Overall, even if the timing and identification of major steps in the shoaling and restriction of the Central American Seaway or  
492 in the uplift of the northern Andes are resolved, the critical threshold for profound changes in atmospheric circulation and  
493 climate may have occurred at any time during the tectonic processes. Within the analyzed time window, large changes in  
494 atmospheric circulation which have been proposed as a response to the closure of the Central American Seaway (Ravelo et al.,  
495 2004) are absent.

496 **5 Conclusions**

- 497 1) Between 4.7 and 4.2 Ma, a permanently humid climate with broad rainforest coverage existed in western equatorial  
498 South America. No evidence was found for a permanent El Niño-like climate state, but strong fluctuations in the  
499 vegetation between 4.7 and 4.55 Ma and between 4.26 and 4.2 Ma indicate strong periodic El Niño variability at this  
500 time. Hydrological changes between 4.55 and 4.26 Ma are attributed to gradual shifts of the Intertropical Convergence  
501 Zone which reached its southernmost position around 4.42 Ma and shifted slightly north afterwards.
- 502 2) The most prominent shift recorded during the early Pliocene is an increase in the representation of the lowland  
503 rainforest around 4.5 Ma.
- 504 3) Between 4.41 and 4.26 Ma, an increased eolian influx of Podocarpaceae pollen indicates an increased strength of the  
505 easterly trade winds, which is presumably related to the shoaling of the EEP thermocline.
- 506 4) Results from proxy data and numerical modelling studies regarding the position of the ITCZ during the early Pliocene  
507 are not necessarily contradictory. Considering the temporal uncertainties regarding major steps of CAS closure and  
508 uplift of the northern Andes, the proposed northward shift of the ITCZ in response to these events might have occurred  
509 much earlier (e.g. during the middle to late Miocene).
- 510 5) The continuous presence of páramo vegetation since 6 Ma implies that the Ecuadorian Andes had already reached an  
511 elevation suitable for the development of vegetation above the upper forest line by the latest Miocene. We present  
512 new paleobotanical evidence indicating an earlier development of páramo vegetation than previously suggested by  
513 terrestrial paleobotanical records.

514

515 **Data availability**

516 The underlying research data are stored in PANGAEA as datasets PANGAEA.884280, PANGAEA.891294 and  
517 PANGAEA.884153, which are combined in PANGAEA.884285 <<https://doi.pangaea.de/10.1594/PANGAEA.884285>>.

518

519 **Author contribution**

520 L. Dupont and F. Grimmer conceived the idea, and L. Dupont, F. Grimmer and F. Lamy carried out the analyses. F. Grimmer  
521 prepared the manuscript with contributions from all co-authors.

522

523 **Competing interests**

524 The authors declare that they have no conflict of interest.

525

526 **Acknowledgements**

527 We thank Carina Hoorn, Jun Tian, Henry Hooghiemstra & Suzette Flantua and an anonymous referee for their insightful  
528 comments on the original manuscript. This project was funded by the Deutsche Forschungsgemeinschaft (DFG) through the  
529 TROPSAP project (DU221/6) and via the DFG Research Center / Cluster of Excellence “The Ocean in the Earth System —  
530 MARUM”. The first author thanks GLOMAR – Bremen International Graduate School for Marine Sciences, University of  
531 Bremen, Germany, for support. The IODP Gulf Coast Repository (GCR) we acknowledge for their assistance in providing the  
532 core samples.

533

534 **References**

535 Anderson, V. J., Saylor, J. E., Shanahan, T. M., and Horton, B. K.: Paleoelevation records from lipid biomarkers:  
536 Application to the tropical Andes, *Geological Society of America Bulletin*, 127, 1604-1616, 2015.  
537 Balslev, H.: Distribution Patterns of Ecuadorean Plant-Species, *Taxon*, 37, 567-577, 1988.  
538 Barnes, J. B., Ehlers, T. A., Insel, N., McQuarrie, N., and Poulsen, C. J.: Linking orography, climate, and exhumation  
539 across the central Andes, *Geology*, 40, 1135-1138, 2012.

540 Bartoli, G., Sarnthein, M., Weinelt, M., Erlenkeuser, H., Garbe-Schönberg, D., and Lea, D. W.: Final closure of  
541 Panama and the onset of northern hemisphere glaciation, *Earth and Planetary Science Letters*, 237, 33-44, 2005.

542 Behling, H., Hooghiemstra, H., and Negret, A. J.: Holocene history of the Choco Rain Forest from Laguna Piusbi,  
543 Southern Pacific Lowlands of Colombia, 1998. 1998.

544 Bendix, A. and Bendix, J.: Heavy rainfall episodes in Ecuador during El Nino events and associated regional  
545 atmospheric circulation and SST patterns, *Advances in Geosciences*, 6, 43-49, 2006.

546 Bendix, J. and Lauer, W.: Die Niederschlagsjahreszeiten in Ecuador und ihre Klimadynamische Interpretation,  
547 1992. 1992.

548 Billups, K., Ravelo, A. C., Zachos, J. C., and Norris, R. D.: Link between oceanic heat transport thermohaline  
549 circulation and the Intertropical Convergence Zone in the early Pliocene Atlantic, *Geology*, 24, 319-322, 1999.

550 Bush, M. B. and Weng, C.: Introducing a new (freeware) tool for palynology, *Journal of Biogeography*, 34, 377-  
551 380, 2007.

552 Cannariato, K. G. and Ravelo, A. C.: Pliocene-Pleistocene evolution of eastern tropical Pacific surface water  
553 circulation and thermocline depth, *Paleoceanography*, 12, 805-820, 1997.

554 Colinvaux, P., De Oliveira, P. E., and Moreno Patino, J. E.: Amazon Pollen Manual and Atlas, 1999.

555 Coltorti, M. and Ollier, C. D.: Geomorphic and tectonic Evolution of the Ecuadorian Andes, *Geomorphology*, 32,  
556 1-19, 2000.

557 Corredor, F.: Eastward extent of the Late Eocene-Early Oligocene onset of deformation across the northern Andes:  
558 constraints from the northern portion of the Eastern Cordillera fold belt, Colombia, *Journal of South American  
559 Earth Sciences*, 16, 445-457, 2003.

560 Fedorov, A. V., Dekens, P. S., McCarthy, M., Ravelo, A. C., deMenocal, P. B., Barreiro, M., Pacanowski, R. C., and  
561 Philander, S. G.: The Pliocene paradox (mechanisms for a permanent El Nino), *Science*, 312, 1485-1489, 2006.

562 Feng and Poulsen, C. J.: Andean elevation control on tropical Pacific climate and ENSO, *Paleoceanography*, 29,  
563 795-809, 2014.

564 Flantua, S., Hooghiemstra, H., Van Boxel, J. H., Cabrera, M., González-Carranza, Z., and González-Arango, C.:  
565 Connectivity dynamics since the last glacial maximum in the northern Andes a pollen driven framework to assess  
566 potential migration. In: *Paleobotany and Biogeography: A Festschrift for Alan Graham in His 80th Year*, W. D.  
567 Stevens, O. M. M., P. H. Raven (Ed.), Missouri Botanical Garden Press, St. Louis, 2014.

568 Flohn, H.: A hemispheric circulation asymmetry during Late Tertiary, *Geologische Rundschau*, 70, 725-736, 1981.

569 Garziona, C. N., Hoke, G. D., Libarkin, J. C., Withers, S., MacFadden, B., Eiler, J., Ghosh, P., and Mulch, A.: Rise of  
570 the Andes, *Science*, 320, 1304-1307, 2008.

571 Gentry, A. H.: Species richness and floristic composition of Chocó region plant communities, *Caldasia*, 15, 71-91,  
572 1986.

573 González, C., Urrego, L. E., and Martínez, J. I.: Late Quaternary vegetation and climate change in the Panama  
574 Basin: Palynological evidence from marine cores ODP 677B and TR 163-38, *Palaeogeography, Palaeoclimatology,  
575 Palaeoecology*, 234, 62-80, 2006.

576 Govin, A., Holzwarth, U., Heslop, D., Ford Keeling, L., Zabel, M., Mulitza, S., Collins, J. A., and Chiessi, C. M.:  
577 Distribution of major elements in Atlantic surface sediments (36°N-49°S): Imprint of terrigenous input and  
578 continental weathering, *Geochemistry, Geophysics, Geosystems*, 13, n/a-n/a, 2012.

579 Gregory-Wodzicki, K. M.: Uplift history of the Central and Northern Andes: A review, *Geological Society of America  
580 Bulletin*, 112, 1091-1105, 2000.

581 Grimm, E.: *Tilia and Tiliagraph*, Illinois State Museum, Springfield, 1991. 1991.

582 Groeneveld, J., Hathorne, E. C., Steinke, S., DeBey, H., Mackensen, A., and Tiedemann, R.: Glacial induced closure  
583 of the Panamanian Gateway during Marine Isotope Stages (MIS) 95-100, *Earth and Planetary Science Letters*,  
584 404, 296-306, 2014.

585 Haug, G. H. and Tiedemann, R.: Effect of the formation of the Isthmus of Panama on Atlantic Ocean thermohaline  
586 circulation, *Nature*, 393, 673-676, 1998.

587 Haug, G. H., Tiedemann, R., Zahn, R., and Ravelo, A. C.: Role of Panama uplift on oceanic freshwater balance,  
588 *Geology*, 29, 207-210, 2001.

589 Hooghiemstra, H.: Vegetational and Climatic History of the High Plain of Bogotá, Colombia: A Continuous Record  
590 of the Last 3.5 Million Years, A.R. Gantner Verlag K.G., Vaduz, 1984.

591 Hooghiemstra, H., Wijninga, V. M., and Cleef, A. M.: The Paleobotanical Record of Colombia: Implications for  
592 Biogeography and Biodiversity<sup>1</sup>, *Annals of the Missouri Botanical Garden*, 93, 297-325, 2006.

593 Hoorn, C.: Andean tectonics as a cause for changing drainage patterns in Miocene northern South America, 1995.  
594 1995.



595 Hoorn, C., Bogotá-A., G. R., Romero-Baez, M., Lammertsma, E. I., Flantua, S., Dantas, E. L., Dino, R., do Carmo, D.  
596 A., and Chemale Jr, F.: The Amazon at sea: Onset and stages of the Amazon River from a marine record, with  
597 special reference to Neogene plant turnover in the drainage basin, *Global and Planetary Change*, 2017. 2017.  
598 Hoorn, C. and Flantua, S.: Geology. An early start for the Panama land bridge, *Science*, 348, 186-187, 2015.  
599 Hoorn, C., Wesselingh, F. P., ter Steege, H., Bermudez, M. A., Mora, A., Sevink, J., Sanmartin, I., Sanchez-Meseguer,  
600 A., Anderson, C. L., Figueiredo, J. P., Jaramillo, C., Riff, D., Negri, F. R., Hooghiemstra, H., Lundberg, J., Stadler, T.,  
601 Sarkinen, T., and Antonelli, A.: Amazonia through time: Andean uplift, climate change, landscape evolution, and  
602 biodiversity, *Science*, 330, 927-931, 2010.  
603 Hovan: Late Cenozoic Atmospheric Circulation Intensity and climatic history recorded by eolian deposition in the  
604 eastern equatorial pacific ocean Leg138, 1995. 1995.  
605 Jørgensen, P. M., León-Yáñez, S., and Missouri Botanical Garden.: Catalogue of the vascular plants of Ecuador =  
606 Catálogo de las plantas vasculares del Ecuador, Missouri Botanical Garden Press, St. Louis, Mo., 1999.  
607 Kaandorp, R. J. G., Wesselingh, F. P., and Vonhof, H. B.: Ecological implications from geochemical records of  
608 Miocene Western Amazonian bivalves, *Journal of South American Earth Sciences*, 21, 54-74, 2006.  
609 Kessler, M.: The "Polylepis problem": Where do we stand?, *Ecotropica*, 8, 97-110, 2002.  
610 Lawrence, K. T., Liu, Z., and Herbert, T. D.: Evolution of the eastern tropical Pacific through Plio-Pleistocene  
611 glaciation, *Science*, 312, 79-83, 2006.  
612 Li, G. and Xie, S. P.: Tropical Biases in CMIP5 Multimodel Ensemble: The Excessive Equatorial Pacific Cold Tongue  
613 and Double ITCZ Problems, *Journal of Climate*, 27, 1765-1780, 2014.  
614 Luteyn, J. L.: Páramos, *Memoirs of The New York Botanical Garden*, 1999.  
615 Maher, L. J.: Nomograms for computing 0.95 confidence limits of pollen data, *Review of Palaeobotany and*  
616 *Palynology*, 13, 85-93, 1972.  
617 Marchant, R., Almeida, L., Behling, H., Berrio, J. C., Bush, M., Cleef, A., Duivenvoorden, J., Kappelle, M., De Oliveira,  
618 P., Teixeira de Oliveira-Filho, A., Lozano-Garcia, S., Hooghiemstra, H., Ledru, M.-P., Ludlow-Wiechers, B.,  
619 Markgraf, V., Mancini, V., Paez, M., Prieto, A., Rangel, O., and Salgado-Labouriau, M.: Distribution and ecology of  
620 parent taxa of pollen lodged within the Latin American Pollen Database, *Review of Palaeobotany and Palynology*,  
621 121, 1-75, 2002.  
622 Marchant, R., Behling, H., Berrio, J. C., Cleef, A., Duivenvoorden, J., Hooghiemstra, H., Kuhry, P., Melief, B., Van  
623 Geel, B., Van der Hammen, T., Van Reenen, G., and Wille, M.: Mid- to Late-Holocene pollen-based biome  
624 reconstructions for Colombia, *Quaternary Science Reviews*, 20, 1289-1308, 2001.  
625 Milliman, J. D. and Farnsworth, K. L.: River discharge to the coastal ocean : a global synthesis, Cambridge  
626 University Press, Cambridge ; New York, 2011.  
627 Mix, A., Tiedemann, R., and Blum, P.: Proceedings of the Ocean Drilling Program, Initial Reports, 202, 2003.  
628 Montes, C., Cardona, A., Jaramillo, C., Pardo, A., Silva, J. C., Valencia, V., Ayala, C., Pérez-Angel, L. C., Rondriguez-  
629 Parra, L. A., Ramirez, V., and Nino, H.: Middle Miocene closure of the Central American Seaway,  
630 *Paleoceanography*, 348, 226-229, 2015.  
631 Mora-Páez, H., Mencin, D. J., Molnar, P., Diederix, H., Cardona-Piedrahita, L., Peláez-Gaviria, J.-R., and Corchuelo-  
632 Cuervo, Y.: GPS velocities and the construction of the Eastern Cordillera of the Colombian Andes *Geophysical*  
633 *Research Letters* Volume 43, Issue 16. In: *Geophysical Research Letters*, 16, 2016.  
634 Mora, A., Parra, M., Strecker, M. R., Sobel, E. R., Hooghiemstra, H., Torres, V., and Jaramillo, J. V.: Climatic forcing  
635 of asymmetric orogenic evolution in the Eastern Cordillera of Colombia, *GSA Bulletin*, 120, 930-949, 2008.  
636 Mulitza, S., Prange, M., Stuu, J. B., Zabel, M., von Dobeneck, T., Itambi, A. C., Nizou, J., Schulz, M., and Wefer, G.:  
637 Sahel megadroughts triggered by glacial slowdowns of Atlantic meridional overturning, *Paleoceanography*, 23,  
638 2008.  
639 Murillo, M. T. and Bless, M. J. M.: Spores of recent Colombian Pteridophyta I Trilete Spores, *Review of*  
640 *Palaeobotany and Palynology*, 1974. 1974.  
641 Murillo, M. T. and Bless, M. J. M.: Spores of recent Colombian Pteridophyta II Monolete Spores, *Review of*  
642 *Palaeobotany and Palynology*, 1978. 1978.  
643 Niemann, H., Brunschön, C., and Behling, H.: Vegetation/modern pollen rain relationship along an altitudinal  
644 transect between 1920 and 3185ma.s.l. in the Podocarpus National Park region, southeastern Ecuadorian Andes,  
645 *Review of Palaeobotany and Palynology*, 159, 69-80, 2010.  
646 O'Dea, A., Lessios, A. H., Coates, A. G., Eytan, R. I., Restrepo-Moreno, S. A., Cione, A. L., Collins, L. S., de Queiroz,  
647 A., Farris, D. W., Norris, R. D., Stallard, R. F., Woodburne, M. O., Aguilera, O., Aubry, M.-P., Berggren, W. A., Budd,  
648 A. F., Cozzuol, M. A., Coppard, S. E., Duque-Caro, H., Finnegan, S., Gasparini, G. M., Grossman, E. L., Johnson, K.  
649 G., Keigwin, L. D., Knowlton, N., Leigh, E. G., Leonard-Pingel, J. S., Marko, P. B., Pyenson, N. D., Rachello-Dolmen,

650 P. G., Soibelzon, E., Soibelzon, L., Todd, J. A., Vermeij, G. J., and Jackson, J. B. C.: Formation of the Isthmus of  
651 Panama, *Science Advances*, 2, 2016.

652 Pak, H. and Zaneveld, J. R.: Equatorial Front in the Eastern Pacific Ocean, *J Phys Oceanogr*, 4, 570-578, 1974.

653 Pettke, T., Halliday, A. N., and Rea, D. K.: Cenozoic evolution of Asian climate and sources of Pacific seawater Pb  
654 and Nd derived from eolian dust of sediment core LL44-GPC3, *Paleoceanography*, 17, 2002.

655 Pisias, N.: Paleoceanography of the eastern equatorial Pacific during the Neogene: Synthesis of Leg 138 drilling  
656 results, *Proceedings of the Ocean Drilling Program, Scientific Results*, 138, 5-21, 1995.

657 Ravelo, A. C., Andreasen, D. H., Lyle, M. W., Lyle, A. O., and Wara, M. W.: Regional climate shifts caused by gradual  
658 global cooling in the Pliocene epoch, 2004. 2004.

659 Regal, P. J.: Pollination by Wind and Animals: Ecology of Geographic Patterns, *Annual Review of Ecology and*  
660 *Systematics*, 13, 497-524, 1982.

661 Richter, T. O., van der Gaast, S., Koster, B., Vaars, A., Gieles, R., de Stigter, H. C., de Haas, H., and van Weering, T.  
662 C. E.: The Avaatech XRF Core Scanner: Technical description and applications to NE Atlantic sediments. In: *New*  
663 *Techniques in Sediment Core Analysis*, Rothwell, R. G. (Ed.), *Geol. Soc. Spec. Publ.*, 2006.

664 Rincon-Martinez, D.: Eastern Pacific background state and tropical South American climate history during the last  
665 3 million years., 2013. *Fachbereich Geowissenschaften, Universität Bremen, Bremen*, 2013.

666 Rincon-Martinez, D., Lamy, F., Contreras, S., Leduc, G., Bard, E., Saukel, C., Blanz, T., Mackensen, A., and  
667 Tiedemann, R.: More humid interglacials in Ecuador during the past 500 kyr linked to latitudinal shifts of the  
668 equatorial front and the Intertropical Convergence Zone in the eastern tropical Pacific, *Paleoceanography*, 25,  
669 2010.

670 Rodbell, D. T., Seltzer, G. O., Anderson, D. M., Abbott, M. B., Enfield, D. B., and Newman, J. H.: An similar to 15,000-  
671 year record of El Niño-driven alluviation in southwestern Ecuador, *Science*, 283, 516-520, 1999.

672 Roubik, D. W. and Moreno, P.: Pollen and spores of Barro Colorado Island [Panama], *Monographs in systematic*  
673 *botany from the Missouri Botanical Garden*, 36, 1991.

674 Salzmann, U., Williams, M., Haywood, A. M., Johnson, A. L. A., Kender, S., and Zalasiewicz, J.: Climate and  
675 environment of a Pliocene warm world, *Palaeogeography, Palaeoclimatology, Palaeoecology*, 309, 1-8, 2011.

676 Sánchez-Baracaldo, P.: Phylogenetics and biogeography of the neotropical fern genera *Jamesonia* and *Eriosorus*  
677 (*Pteridaceae*), *American Journal of Botany*, 91, 274-284, 2004.

678 Schneider, T., Bischoff, T., and Haug, G. H.: Migrations and dynamics of the intertropical convergence zone,  
679 *Nature*, 513, 45-53, 2014.

680 Seilles, B., Goni, M. F. S., Ledru, M. P., Urrego, D. H., Martinez, P., Hanquiez, V., and Schneider, R.: Holocene land-  
681 sea climatic links on the equatorial Pacific coast (Bay of Guayaquil, Ecuador), *Holocene*, 26, 567-577, 2016.

682 Sklenar, P., Duskova, E., and Balslev, H.: Tropical and Temperate: Evolutionary History of Paramo Flora, *Bot Rev*,  
683 77, 71-108, 2011.

684 Sklenar, P. and Jorgensen, P. M.: Distribution patterns of Paramo Plants in Ecuador, *Journal of Biogeography*, 26,  
685 681-691, 1999.

686 Spikings, R. A., Winkler, W., Hughes, R. A., and Handler, R.: Thermochronology of allochthonous terranes in  
687 Ecuador: Unravelling the accretionary and post-accretionary history of the Northern Andes, *Tectonophysics*, 399,  
688 195-220, 2005.

689 Steph, S.: Pliocene Stratigraphy and the impact of Panama Uplift on changes in caribbean and tropical east pacific  
690 upper ocean stratification, 2005. 2005.

691 Steph, S., Tiedemann, R., Groeneveld, J., Sturm, A., and Nürnberg, D.: Pliocene Changes in Tropical East Pacific  
692 Upper Ocean Stratification: Response to Tropical Gateways?, *Proceedings of the Ocean Drilling Program, Scientific*  
693 *Results*, 202, 2006a.

694 Steph, S., Tiedemann, R., Prange, M., Groeneveld, J., Nurnberg, D., Reuning, L., Schulz, M., and Haug, G. H.:  
695 Changes in Caribbean surface hydrography during the Pliocene shoaling of the Central American Seaway,  
696 *Paleoceanography*, 21, 2006b.

697 Steph, S., Tiedemann, R., Prange, M., Groeneveld, J., Schulz, M., Timmermann, A., Nürnberg, D., Rühlemann, C.,  
698 Saukel, C., and Haug, G. H.: Early Pliocene increase in thermohaline overturning: A precondition for the  
699 development of the modern equatorial Pacific cold tongue, *Paleoceanography*, 25, n/a-n/a, 2010.

700 Takahashi, K. and Battisti, D. S.: Processes Controlling the Mean Tropical Pacific Precipitation Pattern. Part I: The  
701 Andes and the Eastern Pacific ITCZ, *Journal of Climate*, 20, 3434-3451, 2007.

702 Tiedemann, R., Sturm, A., Steph, S., Lund, S. P., and Stoner, J. S.: Astronomically calibrated timescales from 6 to  
703 2.5 Ma and benthic isotope stratigraphies, sites 1236, 1237, 1239, and 1241, *Proceedings of the Ocean Drilling*  
704 *Program, Scientific Results*, 202, 2007.

705 Tjallingii, R., Röhl, U., Kölling, M., and Bickert, T.: Influence of the water content on X-ray fluorescence core-  
706 scanning measurements in soft marine sediments, *Geochemistry, Geophysics, Geosystems*, 8, 2007.

707 Twilley, R. R., Cárdenas, W., Rivera-Monroy, V. H., Espinoza, J., Suescum, R., Armijos, M. M., and Solórzano, L.:  
708 The Gulf of Guayaquil and the Guayas River Estuary, Ecuador. In: *Coastal Marine Ecosystems of Latin America*,  
709 Seeliger, U. and Kjerfve, B. (Eds.), Springer, Heidelberg, 2001.

710 Van der Hammen, T.: The Pleistocene Changes of Vegetation and Climate in Tropical South America, *Journal of*  
711 *Biogeography*, 1, 3-26, 1974.

712 Van der Hammen, T., Werner, J. H., and van Dommelen, H.: Palynological record of the upheaval of the Northern  
713 Andes: a study of the Pliocene and Lower Quaternary of the Colombian early evolution of its high-Andean biota,  
714 *Review of Palaeobotany and Palynology*, 16, 1-122, 1973.

715 Vuille, M., Bradley, R. S., and Keimig, F.: Climate variability in the Andes of Ecuador and its relation to tropical  
716 Pacific and Atlantic Sea surface temperature anomalies, *Journal of Climate*, 2000. 2000.

717 Wara, M. W., Ravelo, A. C., and Delaney, M. L.: Permanent El Niño-like conditions during the Pliocene warm  
718 period, *Science*, 309, 758-761, 2005.

719 Zhang, X., Prange, M., Steph, S., Butzin, M., Krebs, U., Lunt, D. J., Nisancioglu, K. H., Park, W., Schmittner, A.,  
720 Schneider, B., and Schulz, M.: Changes in equatorial Pacific thermocline depth in response to Panamanian seaway  
721 closure: Insights from a multi-model study, *Earth and Planetary Science Letters*, 2012. 76-84, 2012.

722 Zhang, Y. G., Pagani, M., and Liu, Z.: A 12-million-year temperature history of the tropical Pacific Ocean, *Science*,  
723 344, 84-87, 2014.

724